

Archaean and Proterozoic crustal evolution in the Eastern Succession of the Mt Isa district, Australia: U–Pb and Hf-isotope studies of detrital zircons*

W. L. GRIFFIN^{1,2†}, E. A. BELOUSOVA¹, S. G. WALTERS^{1,3} AND S. Y. O'REILLY¹

¹GEMOC ARC National Key Centre, Department of Earth and Planetary Sciences, Macquarie University, NSW 2109, Australia.

²CSIRO Exploration and Mining, North Ryde, NSW 2113, Australia.

³GeoDiscovery Group Pty Ltd, PO Box 59, Sherwood, Qld 4075, Australia.

Over 500 zircon grains separated from modern sediments in 10 drainages covering the Eastern Succession of the Mt Isa Inlier have been analysed for U–Pb ages, Hf isotopes, and trace elements, using *in situ* LAM-ICPMS techniques, to evaluate the efficacy of this approach in characterising large-scale crustal evolution. U–Pb age spectra are used to estimate the timing of terrane-scale events, primarily magmatic episodes; Hf isotopes provide information on the relative contributions of juvenile material and reworked older crust at each stage of crustal evolution; trace-element patterns of zircons are used to characterise original magma types. The integration of these data for individual zircon grains produces an event signature that provides more information than that gained from U–Pb dating alone. The data define four major stages of crustal evolution in the area: 2550–2330 Ma, 1950–1825 Ma, 1800–1600 Ma, and 1590–1420 Ma. Each stage, except the last, involved crustal extension, and ended with a period of crustal homogenisation, which is reflected in the isotopic composition of magmatic rocks generated by crustal reworking in the succeeding stage. Reworking of Neoproterozoic crust contributed significantly to crustal magmatism throughout the Proterozoic history. A major input of juvenile mafic material around 1625 Ma (interpreted as the magmatic age of the Toole Creek Volcanics) is poorly represented in the database of conventional geochronology but is prominent in the detrital zircon record. The major late-stage granitic magmatism of the Williams and Narku Batholiths (1520–1490 Ma) was generated almost entirely from older crust, with little juvenile input. The study demonstrates that sampling of carefully selected modern drainages and the analysis of statistically large numbers of detrital zircons can provide insights additional to those gained from conventional analysis of U–Pb and Sm–Nd systematics in selected rock samples. The integrated use of U–Pb age, Hf-isotope composition and trace-element patterns in detrital zircons is a powerful and relatively inexpensive tool for the analysis of terrane-scale crustal evolution, and for the correlation of terranes.

KEY WORDS: detrital zircon, event signature, Hf isotopes, Mt Isa, uranium–lead dating.

INTRODUCTION

The Mt Isa block is a large segment of Palaeoproterozoic to Mesoproterozoic continental crust in northwest Queensland (Figure 1). It has been extensively studied because of its significant metallogenic endowment; it is the site of several large operating mines, and of intense current exploration activity. It is conveniently divided into three major units: the Western and Eastern Successions (or Fold Belts), divided by an older Central Belt (Kalkadoon–Leichhardt Belt) (Figure 1). Much current research and mineral exploration activity is focused on the Eastern Succession, and especially the

Soldiers Cap Group (part of the Maronan Supergroup: Figure 2), a package of *ca* 1712–1655 Ma metasupracrustal rocks that hosts the world-class Cannington Ag–Pb–Zn deposit and several iron oxide Cu–Au deposits (e.g. Ernest Henry, Eloise). Despite this level of research, the relationships of the Soldiers Cap Group to other sequences in the Eastern Succession, and to the rest of the Mt Isa block, remain debatable. Lithostratigraphic correlations within the Maronan Supergroup itself are not well defined and are complicated by variations in metamorphic grade and poor outcrop.

Given the economic importance of the region, a significant amount of U–Pb zircon dating has been

Appendix 2 [indicated by an asterisk (*) in the text and listed at the end of the paper] is a Supplementary Paper; copies may be obtained from the Geological Society of Australia's website (www.gsa.org.au) or from the National Library of Australia's Pandora archive (<<http://nla.gov.au/nla.arc-25194>>).

†Corresponding author: bill.griffin@mq.edu.au

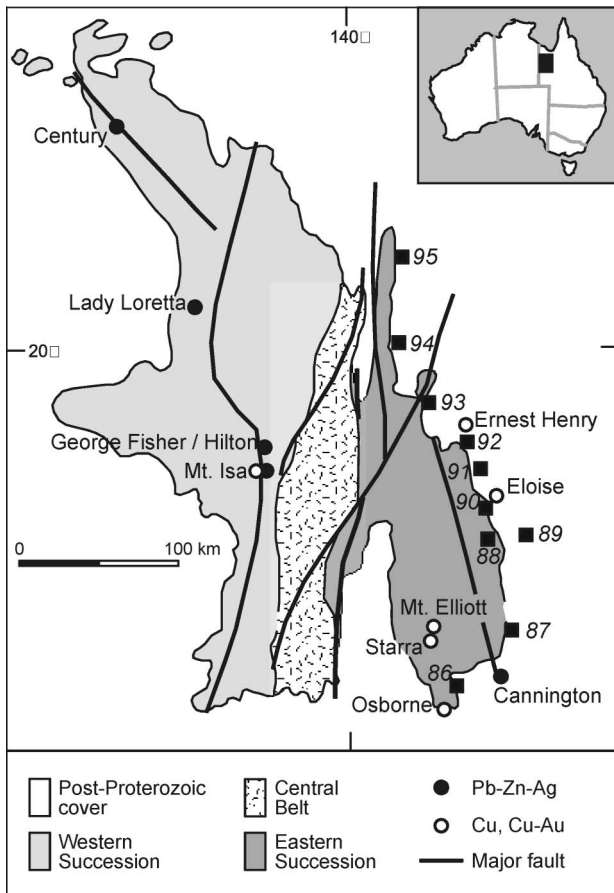


Figure 1 Map showing the geological setting of the Eastern Succession, with sampling points.

carried out in the Eastern Succession to support mapping, mineral exploration and research initiatives (Page & Sun 1998 and references therein; Giles & Nutman 2003). This geochronological framework is an important component in the characterisation of geological evolution and correlation of events. However, it does not answer fundamental questions about the nature of these events, such as the degree of crustal recycling or the importance and timing of juvenile (mantle-derived) contributions to the crust. Without this information, it is difficult to evaluate the overall processes of crustal evolution, to understand which aspects of crustal evolution have been responsible for the metallogenic endowment, or to decipher the tectonic relationships between the Soldiers Cap Terrane and the rest of the Mt Isa block.

The traditional approach to this problem relies on the dating of individual (usually igneous) rock units by U–Pb or other techniques, combined with the determination of initial $^{87}\text{Sr}/^{86}\text{Sr}$ and/or $^{143}\text{Nd}/^{144}\text{Nd}$ ratios, or whole-rock Pb–Pb data, to evaluate the nature of the source for each magma. This approach can be hampered by the disturbance of Rb/Sr and Sm/Nd whole-rock systematics by metamorphism, as demonstrated by the intense controversy over the interpretation of even small areas such as Isua in west Greenland (Bennett *et al.* 1993; Blichert-Toft *et al.* 1999; Vervoort & Blichert-Toft 1999; Polat *et al.* 2003). The time and expense

involved in acquiring U–Pb and Nd-isotope data on significant numbers of samples also limit its application to large-scale crustal-evolution studies, including correlation between terranes.

However, recent advances in laser ablation microprobe ICPMS (LAM-ICPMS) make it possible to obtain *in situ* U–Pb age data comparable in quality with ion microprobe analyses from single zircon grains (Horn *et al.* 2000; Belousova *et al.* 2001; Andersen *et al.* 2002; Jackson *et al.* 2004). These data are generated quickly (~5 minutes/grain) and at a relatively low unit cost, making it feasible to analyse large populations. The analysis of such populations sampled in modern drainage sediments generates U–Pb age spectra that can be used to date fundamental terrane-scale events—magmatic episodes, metamorphism and hydrothermal activity—and to constrain sedimentary provenance.

High-precision *in situ* analysis of Hf isotopes in zircon by LAM-ICPMS techniques (Griffin *et al.* 2000) provides additional information on magma sources (Knudsen *et al.* 2001; Griffin *et al.* 2004). In terms of isotopic systematics, the Lu–Hf system behaves analogously to the more widely used Sm–Nd system; studies on a whole-rock scale have demonstrated a close coherence between the two systems in crustal rocks (see summary by Vervoort *et al.* 1999). The low Lu/Hf of zircon means that the zircon essentially preserves the initial $^{176}\text{Hf}/^{177}\text{Hf}$ of the magma from which it crystallised. Because zircon is extremely refractory and represents the major reservoir of Hf in most rocks, it also is very resistant to resetting of the Hf-isotope composition during metamorphic or even magmatic events. This makes the analysis of Hf isotopes in single zircons a powerful tool for crustal evolution studies.

The development of trace-element discriminants that relate zircon composition to host-rock composition provides a further layer of information, by allowing a statistically based evaluation of the parent rock type of each grain (Belousova *et al.* 2002; Griffin *et al.* 2004). The integrated U–Pb, Hf-isotope, and trace-element characterisation of large zircon populations (the *TerraneChron* approach: O'Reilly *et al.* 2004) therefore can be used to define terrane-scale event signatures that represent patterns of crustal evolution within a geochronological framework.

In this study, we have applied this approach to a series of samples from streams that drain the Soldiers Cap Group and the igneous rocks that intrude it. We use the data to assess: (i) the ability of this approach to capture known geological and geochronological relationships; (ii) the relative importance of crustal recycling and juvenile mantle input during the evolution of the Soldiers Cap Group and the production of the late granitoid batholiths of the Eastern Succession; (iii) stratigraphic equivalencies within the Eastern Succession; and (iv) the relationship of the Soldiers Cap Group to the rest of the Mt Isa block. The results demonstrate that this approach reproduces the previously known geochronological framework of the Eastern Succession. However, it also adds significant new information on the timing and distribution of several igneous events, on the nature and age of the deep crust, and on the long-term crustal evolution of the

region. Finally, we show that a complex history of crustal evolution stretching back into the Archaean can be reconstructed using detrital zircons recycled from younger sediments.

REGIONAL GEOLOGICAL FRAMEWORK

Overview

The Mt Isa Inlier is divided into three major lithostratigraphic and structural terranes: the Western and Eastern Successions (fold belts), separated by the older central Kalkadoon–Leichhardt Belt (Figure 1). The terranes are characterised by sequences of variably deformed and metamorphosed Palaeoproterozoic to Mesoproterozoic sedimentary, volcanic and intrusive rocks deposited in basins related to partly superimposed ensialic rifting events (Blake 1987; Beardsmore *et al.* 1988; O’Dea *et al.* 1997; Scott *et al.* 2000; McLaren & Sandiford 2001; Betts *et al.* 2006). Within this framework, two major Proterozoic cycles are recognised. The earlier one is represented by restricted areas of Palaeoproterozoic supracrustal rocks, deformed and metamorphosed during the Barramundi Orogeny (*ca* 1900–1870 Ma); the basement to this succession is poorly known. The second cycle is characterised by the development and deformation of three stacked and superimposed superbasins (Leichhardt, Calvert and Isa) that evolved between *ca* 1800 and 1595 Ma, in a regime of high heat flow, repeated magmatism and basin inversion (see review by Betts *et al.* 2006 and references therein). The basin development was terminated by the 1600–1500 Ma Isan Orogeny, which involved major metamorphic episodes at *ca* 1585 Ma (M1: Page & Sun 1998; Giles & Nutman 2002, 2003; Hand & Rubatto 2002) and *ca* 1530 Ma (Connors & Page 1995). Large volumes of felsic rocks were intruded from *ca* 1560 to 1490 Ma.

The current understanding of the lithostratigraphic and geochronological framework of the Mt Isa Inlier, based on decades of mapping and research supported by conventional and SHRIMP U–Pb zircon dating, is indicated in Figure 2. Felsic volcanics and granites are particularly amenable to U–Pb zircon dating and have therefore provided many of the critical ages in this framework. Dating of the metasedimentary rocks that are the dominant components of some sequences has proven more difficult and involves characterisation of provenance and constraints on maximum depositional ages rather than absolute crystallisation ages (Page *et al.* 2000).

In the Eastern Succession, the basal rocks of the Leichhardt Superbasin (*ca* 1790–1730 Ma) are the sedimentary rocks and felsic volcanic rocks of the Argylla Formation; these are overlain by sedimentary rocks and mafic volcanic rocks of the Marraba Volcanics and Mitakoodi Quartzite developed at a mature stage of rifting (Potma & Betts 2006). Post-rift rocks include the carbonate rocks of the Doherty and Corella Formations. In the Calvert Superbasin (1730–1670 Ma) rift-related turbidites, basalts and dolerites of the Kuridala and Llewellyn Creek Formations and Mt Norna Quartzite make up the Soldiers Cap Group, part

of the Maronan Supergroup (Beardsmore *et al.* 1988) (Figure 2). The depositional hiatus that separates the Calvert and Isa Superbasins in the Western Succession is not observed in the Eastern Succession, and the Soldiers Cap Group (Maronan Supergroup) extends up into the Isa Superbasin (*ca* 1670–1590 Ma). The mafic Toole Creek Volcanics in the upper part of the Soldiers Cap Group have a maximum age of *ca* 1658 Ma, based on zircons from interbedded cherts (Page 1988); data presented below suggest that the volcanic rocks are somewhat younger (*ca* 1625 Ma). This is similar to an age for the felsic and igneous rocks of the Tommy Creek Volcanics in the Isa Superbasin (Page & Sun 1998).

Soldiers Cap Group

The Soldiers Cap Group in the Eastern Succession was chosen as the focus of the current study because of its association with economically significant Broken Hill-type (Cannington) and iron oxide Cu–Au (e.g. Ernest Henry, Osborne: Figure 1) mineralisation, and the possibility that it represents an allochthonous terrane with respect to the rest of the Mt Isa Inlier (Beardsmore *et al.* 1988); although broadly coeval, these may not share the same crustal evolution history. Correlations within the Soldiers Cap Group are also poorly defined due to variations in metamorphic grade and the lack of acid volcanic units.

The dominant lithologies of the Soldiers Cap Group in the main outcropping region around Cloncurry (Derrick *et al.* 1976) are upper greenschist to lower amphibolite facies siliciclastics that include planar-bedded pelitic slate and schist, immature meta-arenite and orthoquartzite with graded bedding, and basic volcanic rocks including high-level sills. Thin horizons of banded iron-formation and quartz–gahnite units occur at restricted stratigraphic horizons in association with Broken Hill-type mineralisation (Walters 1998). South of Cloncurry, the metamorphic grade increases to upper amphibolite facies, resulting in dominant migmatitic sillimanite–K-feldspar-bearing gneiss and amphibolite. In conjunction with poor outcrop, this has created difficulties in correlation between the higher metamorphic grade ‘undifferentiated Soldiers Gap Group’ and the stratigraphic subdivisions defined in the Cloncurry region (Blake & Stewart 1992).

Beardsmore *et al.* (1988) presented a lithostratigraphic revision of the Eastern Succession, in which the Soldiers Cap Group in the Cloncurry region as defined by Derrick *et al.* (1976) was assigned to an upper sequence of the proposed Maronan Supergroup. The higher grade metamorphic sequences previously mapped as ‘undifferentiated Soldiers Gap Group’ were assigned to the Fullarton River Group in the lower Maronan Supergroup (Figure 3). Although Beardsmore *et al.* (1988) regarded the Maronan Supergroup as probably older than rift sequences elsewhere in the Mt Isa Inlier, subsequent U–Pb zircon dating (Page 1993; Page & Sun 1998) demonstrated broad age equivalence with cover sequence 3 of Blake (1987) (*ca* 1690–1600 Ma). Given the problems of a proposed lithostratigraphy that appears in part to represent variations in

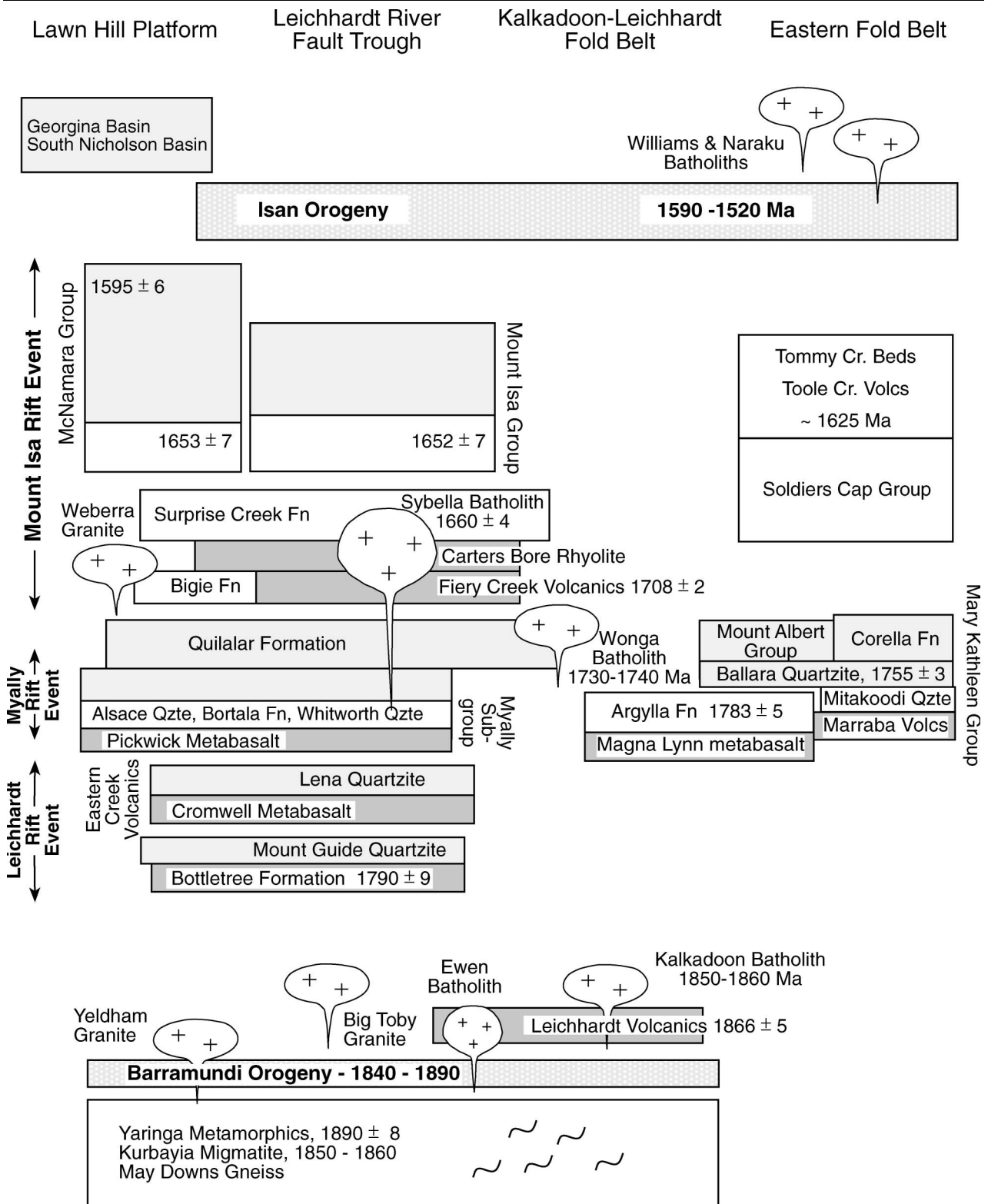


Figure 2 Geochronological framework of the Mt Isa region (modified after McLaren & Sandiford 2001, with geochronological data from Page & Sun 1998).

metamorphic grade, detailed correlations within the Maronan Supergroup remain poorly constrained, and the proposed Soldiers Cap and Fullarton River Groups may include temporal equivalents.

Granites emplaced into the Eastern Succession include deformed granites within the Soldiers Cap

Group (Maramungee Granite Suite, *ca* 1545 Ma), and the extensive Williams–Naraku Batholiths (1530–1500 Ma). The main late to post-tectonic plutons of the Williams–Naraku Batholiths are composed of A-type granitoids dominated by granodiorite and alkali-feldspar granites (Mark 2001). Late orogenic shear zones,

		Stratigraphic Unit		Lithologies	Metamorphic Grade
MARONAN SUPERGROUP	Soldiers Cap Group	Toole Creek Volcanics		Amphibolite, carbonaceous slate, scapolitic siltstone	Middle greenschist
		Mount Norna Quartzite		Feldspathic psammite, thin pelite, minor calc-silicate <i>Thin BIF's</i>	Upper greenschist
		Llewellyn Creek Formation		Bedded quartz-mica psammite and pelite with graded turbidic cycles	Lower amphibolite
	Fullarton River Group	New Hope Arkose	Glen Idol Schist	Thickly bedded quartzo-feldspathic psammite with partial melting	Lower amphibolite
		Upper Gandry Dam Gneiss		Psammopelitic gneiss, leucogneiss, granite gneiss, amphibolite <i>Thin BIF's and gahnite 'quartzites'</i>	Middle amphibolite
		Lower Gandry Dam Gneiss		Migmatitic psammopelitic gneiss, feldspathic psammite, amphibolite <i>Thin BIF's and gahnite 'quartzites'</i>	Upper amphibolite

Figure 3 Correlations within the Soldiers Cap Group (modified from Beardsmore *et al.* 1988).

broadly contemporaneous with early intrusive phases of the Williams–Naraku Batholiths, separate areas of different metamorphic grade and controlled regionally extensive sodic–calcic alteration. Continued hydrothermal activity related to late orogenic granitoids and ductile–brittle transitions as the terrane unroofed is associated with a range of iron oxide Cu–Au associated styles of alteration and mineralisation (Williams 1998).

SAMPLING STRATEGY

Ten heavy-mineral samples were collected along the fold belt, from the northern part of the Boomarra Horst to southwest of Cannington, covering the main outcrop extent of the mapped Soldiers Cap Group and adjacent units. The locations of these samples (Appendix 1), their catchment areas, and their relationship to the geology are indicated in Figure 4. Samples were collected as ~2 mm material from heavy-mineral trap sites with sample weights in the order of 20–30 kg. The catchment size is generally in the order of 100 km², and in many instances sample sites were composited (two or three per sample) to give the required coverage of geology. The sampling coverage represents catchment areas within the Soldiers Cap Group with the potential to address key relationships. These areas fall into four main groups.

1. *Boomarra Horst* (samples P9695, 9694, 9693): mapped as ‘undifferentiated Soldiers Cap Group’ on the basis of lithology, although there are some indications from limited dating (Page & Sun 1998) that the sequence may be older.

2. *Cloncurry area* (samples P9692, 9691, 9690): the ‘classic’ outcropping Llewellyn Creek Formation, Mt Norna Quartzite and Toole Creek Volcanics units of the

Soldiers Cap Group, at lower amphibolite – upper greenschist metamorphic facies. The area includes the enigmatic Gilded Rose breccias that may represent diapirism, décollement, and metasomatism along thrust surfaces localised on evaporites in the Mary Kathleen Group (Ryburn *et al.* 1988).

3. *Fullarton River zone* (samples 9689, 9688, 9687): shown on existing mapping as ‘undifferentiated Soldiers Cap Group’. The stratigraphy has been assigned to the Fullarton River Group (Figure 2). This contains the inferred host equivalents of the non-outcropping Cannington deposit (Gandry Dam Gneiss) and older foliated granites (e.g. Maramungee Granite, drained by P9687 catchment). The P9688 catchment also includes part of the Doherty Formation, a zone of metasomatism developed along the contact between the Mary Kathleen Group and the Soldiers Cap Group, and a large area of the Williams Batholith.

4. *Area west of Cannington* (sample P9686): a single sample was taken west of Cannington in a very large drainage covering part of the Mary Kathleen Group and the Williams Batholith.

ANALYTICAL METHODS

Mineral separations were carried out at CSIRO Exploration and Mining, North Ryde. Samples were split and sieved, and heavy minerals ($D > 2.5 \text{ g/cm}^3$) were extracted from subsamples weighing several kilograms using dense media. Magnetic phases were removed using a hand magnet and roll magnetic separator. Zircons were picked from this simple heavy-mineral concentrate under a Leica UV microscope, mounted in 25 mm epoxy resin discs and polished to reveal internal sections. In most cases, we used the 150–250 μm size fraction, which provided zircons large enough for multiple analyses. Over 550

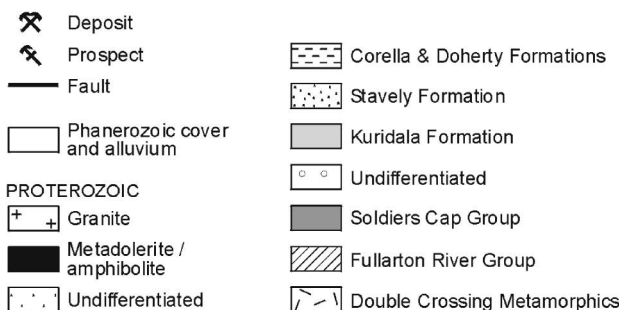
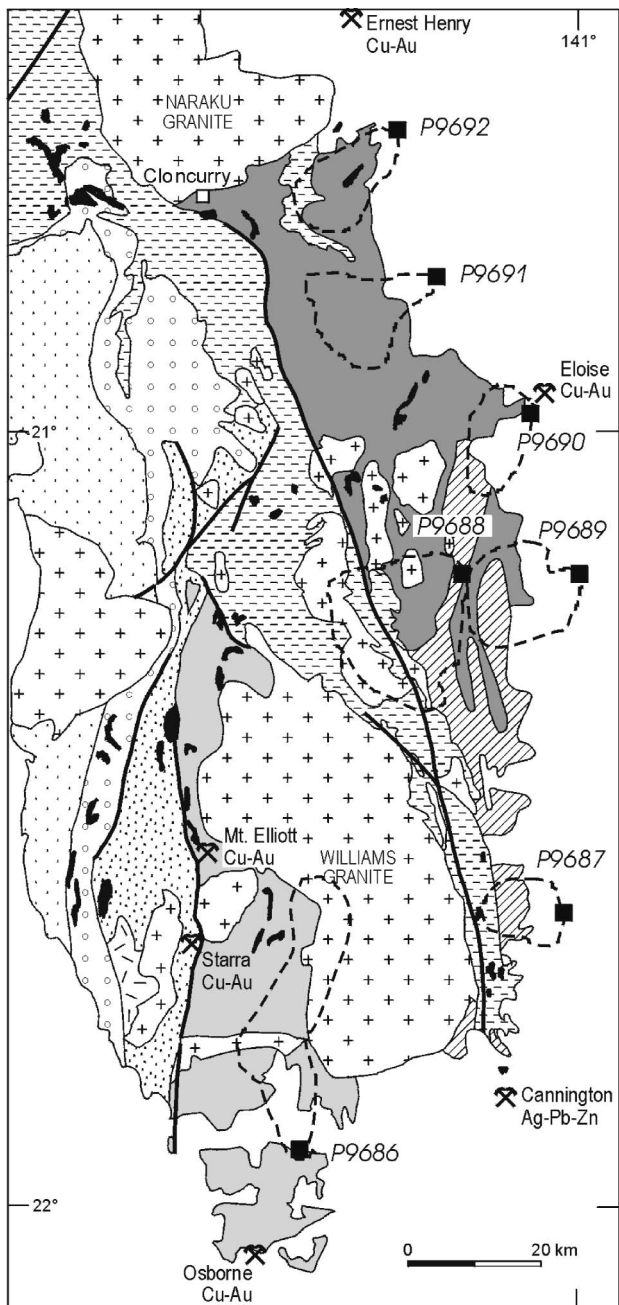


Figure 4 Geological map of the southern part of the Eastern Succession, showing sampled drainages (dashed outlines).

individual grains were imaged in the GEMOC CAME-BAX SX50 electron microprobe (EMP) using back-scattered electron/cathodoluminescence (BSE/CL)

techniques; images were captured digitally using a LINK analysis system. From these images (Figure 5), each grain was classified in terms of its shape, degree of abrasion, and internal structure (Appendix 2*). The electron probe also was used to analyse each grain for Hf, Y, U and Th contents, in the spot selected for U–Pb analysis.

U–Pb dating

Grain mounts containing the samples and 02123 zircon standard were cleaned in 2N nitric acid for ~1 hour prior to analysis. LAM-ICPMS analyses were performed using a custom built UV LAM (Norman *et al.* 1996) coupled to an Agilent 4500, series 300, ICPMS at the GEMOC Key Centre, Macquarie University (Table 1). The analytical techniques and operating conditions are described in detail by Belousova *et al.* (2001) and Jackson *et al.* (2004). Samples and standard were ablated in He, which improves sample transport efficiency, results in more stable signals and gives more reproducible Pb/U fractionation. Ablation pit diameter was generally about 50 μm . Samples were analysed in separate runs of 20 analyses comprising 12 analyses of unknowns bracketed by four analyses of the 02123 zircon standard, a gem-quality zircon from a Norwegian syenite (Ketchum *et al.* 2001).

Raw data were processed using the GLITTER online data-reduction program (see <www.es.mq.edu/GEMOC>). The time-resolved ratios for each analysis were carefully examined for isotopic heterogeneity within the ablation volume (e.g. zones of Pb loss or common Pb related to fractures or areas of radiation damage, inclusions, inherited cores, etc.). Optimal signal intervals for the background and ablation data were selected for each sample and automatically matched with identical time intervals for the standard zircon analyses, thus correcting for the effects of ablation/transport-related U/Pb fractionation and mass bias of the mass spectrometer.

Correction for common-Pb contamination is difficult in LAM-ICPMS analysis because the very low ^{204}Pb signal cannot be measured precisely enough to make a meaningful correction. The effect of common Pb is to increase the $^{207}\text{Pb}/^{206}\text{Pb}$ age of the sample; typical levels of common Pb in ion-probe analysis are $\ll 1\%$ of total Pb and the associated age correction for Proterozoic samples is ≤ 10 million years. The presence of a significant common Pb component also raises the $^{208}\text{Pb}/^{232}\text{Th}$ age, and $^{208}\text{Pb}/^{232}\text{Th}$ ages \gg $^{206}\text{Pb}/^{238}\text{U}$ ages may indicate either common Pb contamination or the differential mobilisation of U–Th–Pb. In the dataset used here, we have rejected grains where the $^{208}\text{Pb}/^{232}\text{Th}$ age is higher than the $^{206}\text{Pb}/^{238}\text{U}$ age by 4σ , unless they showed near-concordance of $^{206}\text{Pb}/^{238}\text{U}$ and $^{207}\text{Pb}/^{235}\text{U}$ ages; such concordance is not produced by any combination of common-Pb and Pb-loss mechanisms.

The external precision and accuracy obtained with this technique are illustrated by comparison with TIMS data for some well-characterised zircons (Table 2). The lack of a significant common-Pb effect is demonstrated by the concordance of LAM-ICPMS U–Pb ages on young

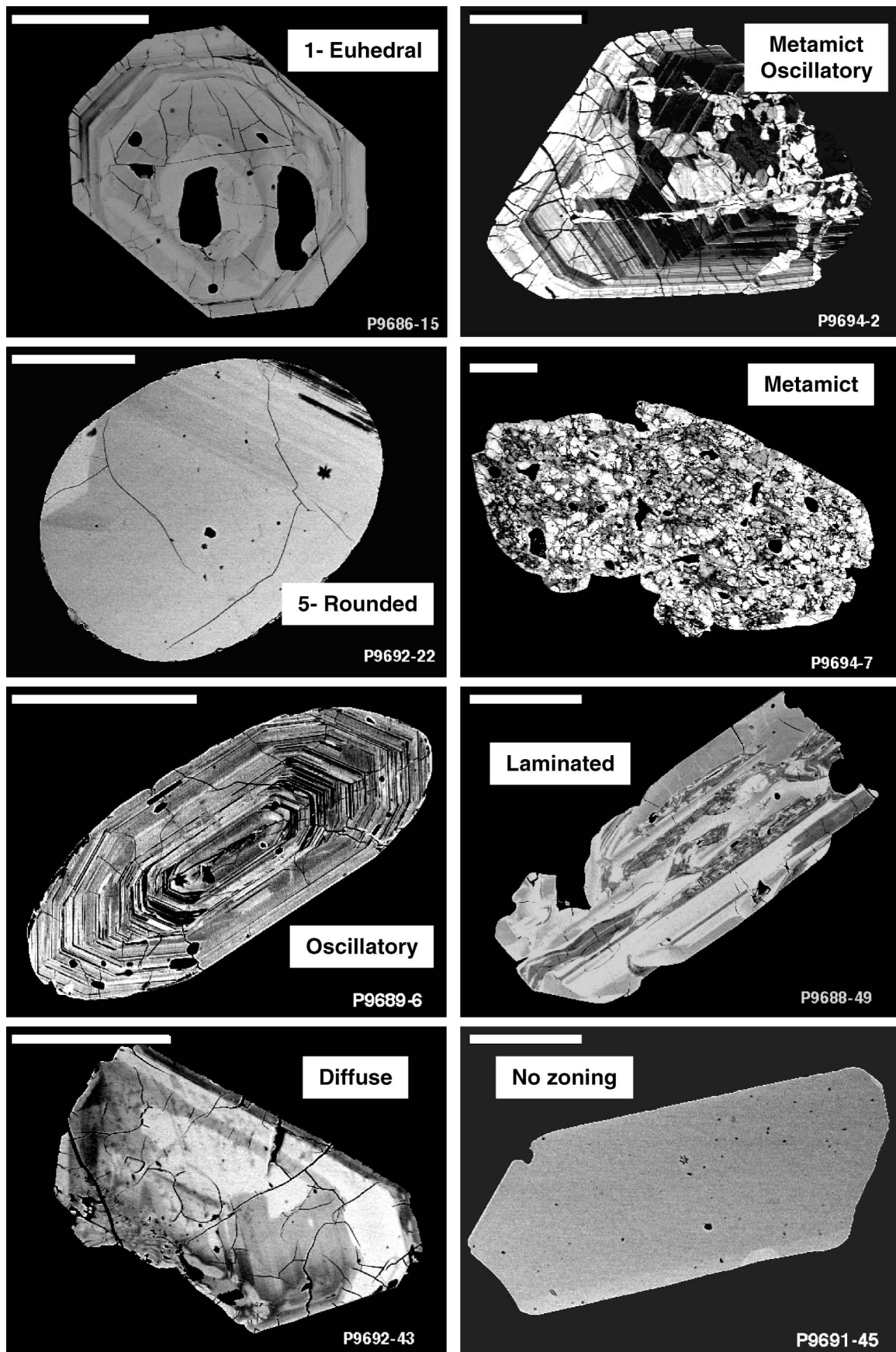


Figure 5 Backscattered electron/cathodoluminescence images of representative zircons, showing features used to classify external form (showing end members of classes 1–5) and internal structure (Appendix 2*). Scale bar: 100 μm .

zircons with those determined by high-precision TIMS analysis. This methodology gives $^{206}\text{Pb}/^{238}\text{U}$ and $^{207}\text{Pb}/^{206}\text{Pb}$ ages with a precision and accuracy comparable with that of most ion-probe data.

Hf-isotope determination

The Hf-isotope analyses reported here were carried out *in situ* using a Merchantek/ New Wave Research LUV266 laser-ablation microprobe, attached to a Nu Plasma multicollector ICPMS, at Macquarie University. The methods are described in detail by Griffin *et al.* (2000, 2004). Most analyses reported here were carried out with a beam diameter of $\sim 60\ \mu\text{m}$, a 4 Hz repetition rate, and a laser power of 2–4 mJ/pulse. This typically gave total Hf signals of $2\text{--}4 \times 10^{-11}\ \text{A}$. Typical ablation times were 30–120 s. Ar carrier gas transported the ablated sample from the laser-ablation cell via a mixing chamber to the ICPMS torch.

Masses 172, 175, 176, 177, 178, 179, and 180 were measured in Faraday cups; all analyses were carried out in static-collection mode. Data are normalised to

$^{179}\text{Hf}/^{177}\text{Hf} = 0.7325$, using an exponential correction for mass bias. The reproducibility of the Hf-isotope analyses has been demonstrated by analyses of solutions of the JMC475 Hf standard (Griffin *et al.* 2004). The typical within-run precision on these solution analyses is ± 0.000015 (2SE). Our mean value for $^{176}\text{Hf}/^{177}\text{Hf}$ is identical to the recommended value (0.28216) of Nowell *et al.* (1998).

Interference of ^{176}Lu on ^{176}Hf is corrected by measuring the intensity of the interference-free ^{175}Lu isotope and using $^{176}\text{Lu}/^{175}\text{Lu} = 0.02669$ (DeBievre & Taylor 1993) to calculate $^{176}\text{Lu}/^{177}\text{Hf}$. Similarly, the interference of ^{176}Yb on ^{176}Hf has been corrected by measuring the interference-free ^{172}Yb isotope and using $^{176}\text{Yb}/^{172}\text{Yb}$ to calculate $^{176}\text{Yb}/^{177}\text{Hf}$. The appropriate value of $^{176}\text{Yb}/^{172}\text{Yb}$ was determined by spiking the JMC475 Hf standard with Yb, and finding the value of $^{176}\text{Yb}/^{172}\text{Yb}$ (0.58669) required to yield the value of $^{176}\text{Hf}/^{177}\text{Hf}$ obtained on the pure Hf solution. Analyses of standard zircons (Griffin *et al.* 2000, 2002, 2004) illustrate the precision and accuracy obtainable on the $^{176}\text{Hf}/^{177}\text{Hf}$ ratio, despite the severe corrections on ^{176}Hf . The typical 2SE precision on the $^{176}\text{Hf}/^{177}\text{Hf}$ ratios presented here is ± 0.00002 , equivalent to $\pm 0.7\ \epsilon_{\text{Hf}}$ unit. The accuracy and precision of the method are discussed in further detail by Griffin *et al.* (2000, 2002, 2004).

The measured $^{176}\text{Lu}/^{177}\text{Hf}$ ratios of the zircons have been used to calculate initial $^{176}\text{Hf}/^{177}\text{Hf}$ ratios. These age corrections are very small, and the typical uncertainty on a single analysis of $^{176}\text{Lu}/^{177}\text{Hf}$ ($\pm 1\%$) contributes an uncertainty of $< 0.05\ \epsilon_{\text{Hf}}$ unit. For the calculation of ϵ_{Hf} values, representing the per mil difference between the sample and the chondritic reservoir (CHUR) at the time of intrusion, we have adopted a decay constant for ^{176}Lu of $1.93 \times 10^{-11}\ \text{y}^{-1}$ and the chondritic values of $^{176}\text{Hf}/^{177}\text{Hf}$ and $^{176}\text{Lu}/^{177}\text{Hf}$ derived by Blichert-Toft and Albarède (1997). Values of ϵ_{Hf} and T_{DM} calculated using recently proposed alternative values of the decay constant for ^{176}Lu are given in Appendix 2*; the use of these values would not affect any of the conclusions given here.

Depleted-mantle model ages (T_{DM}) were calculated using the measured $^{176}\text{Lu}/^{177}\text{Hf}$ ratios, referred to a model depleted mantle with a present-day $^{176}\text{Hf}/^{177}\text{Hf} = 0.28325$, similar to that of average MORB (Nowell *et al.* 1998) and $^{176}\text{Lu}/^{177}\text{Hf} = 0.0384$ (Griffin *et al.* 2000); this is similar, though not identical, to the depleted mantle curve defined

Table 1 Operating conditions and data-acquisition parameters for laser ablation ICPMS microprobe.

ICP-MS	
Model	HP 4500 (Series 300)
Forward power	1350 KW
Gas flows:	
Plasma	Ar 13 L/min
Auxilliary	Ar 0.8 L/min
Carrier	He ca. 1 L/min
LAM	
Wavelength	266 nm
Repetition rate	10 Hz
Pulse duration (FWHM)	6 ns
Focusing objective	10 \times , UV laser achromat, f.l. = 20 mm
Degree of defocusing	200 μm (above sample)
Measured pulse energy	ca 0.5–0.9 mJ
Data-acquisition parameters	
Data-acquisition protocol	Time-resolved analysis
Scanning mode	Peak hopping, 1 point per peak
Isotopes determined	^{206}Pb , ^{207}Pb , ^{208}Pb , ^{232}Th , ^{238}U
Dwell times	15 ms, except ^{207}Pb 20 ms

Table 2 Precision and accuracy obtained by LAM-ICPMS compared with TIMS data on several well-characterised zircons.

Zircon	TIMS $^{207}\text{Pb}/^{206}\text{Pb}$	$^{206}\text{Pb}/^{238}\text{U}$	mswd	$^{207}\text{Pb}/^{235}\text{U}$	mswd	$^{207}\text{Pb}/^{206}\text{Pb}$	mswd
UQ-Z5	1143 \pm 1	Machado and Gauthier (1996) $n = 9$					
$n = 33$ (this work)		1136 \pm 14	4.7	1134 \pm 11	5	1135 \pm 9	6.2
Mud Tank	734 \pm 32	Black and Gulson (1978) $n = 5$					
$n = 42$ (this work)		731 \pm 3^a	1.6	729 \pm 3	1.3	724 \pm 12	1.6
$n = 359$ (long term ^b)		732 \pm 1.4		733.9 \pm 1.1		738.8 \pm 1.7	

^aLAM-ICPMS 206/238 ages preferred for samples with age < 1 Ga and 207/206 ages preferred for older samples.

^bData from Jackson *et al.* (2004).

n , Number of analyses done during different analytical sessions.

by juvenile rocks through time (Vervoort & Blichert-Toft 1999). These T_{DM} ages represent a minimum age for the source of the host magma of the zircon.

DATA TREATMENT AND PRESENTATION

Uranium–lead data

U–Pb data for two typical samples are presented in Figure 6. Since each grain must be treated as a single sample, many grains were analysed that probably would be rejected in conventional ion-probe dating work, because the BSE/CL images suggest alteration, metamict structures or fracturing. As a result, these plots contain a larger proportion of non-concordant grains than is commonly seen in dating reports. The calculation of $^{207}\text{Pb}/^{206}\text{Pb}$ ages for such grains introduces larger errors than for near-concordant grains, and any cracks are likely sites for common Pb deposited by circulating fluids. We therefore have rejected 93 grains (~20%)

that were more than 50% discordant, and/or showed evidence of significant common-Pb contamination.

Age spectra and event definition

The cleaned data are presented as probability density spectra (Ludwig 2000) (Figures 7, 8), which are essentially smoothed histograms that account for the analytical uncertainties on each point. The interpretation of these plots in terms of geological events can be approached in two ways. One is that used in the dating of individual rocks, where the aim is to define a specific instantaneous event, such as the crystallisation of a magmatic rock, and the analytical data are winnowed down to the point where the grains used are within analytical uncertainty of one another or, where spread beyond this level of uncertainty, can be explained by geological arguments.

In the analysis of detrital zircon populations from a wider district, this approach is not appropriate, because the intrusion of a series of magmatic rocks making up a

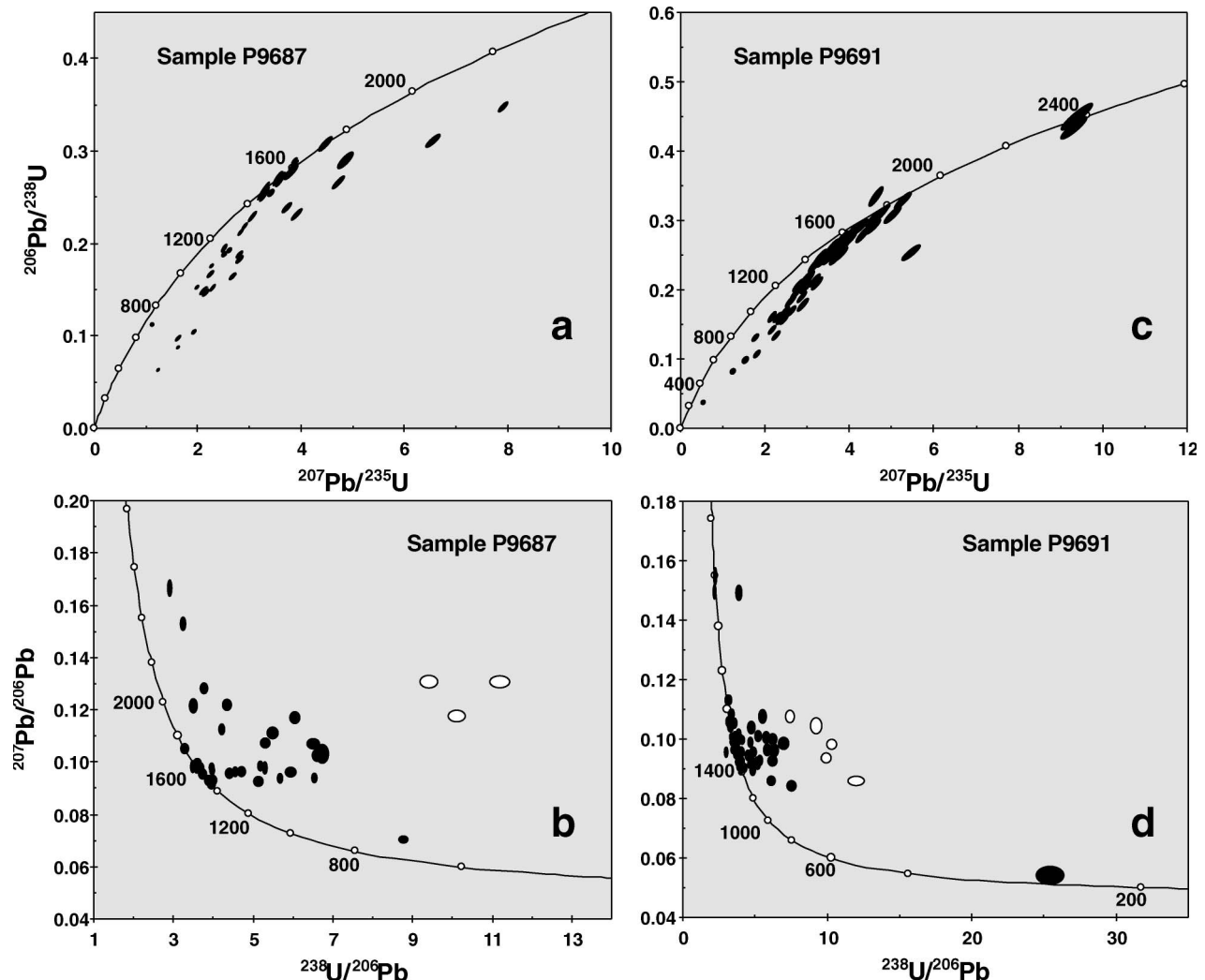


Figure 6 U–Pb data for two representative samples, in Concordia (a, c) and inverse Concordia (Tera–Wasserburg) plots (b, d). Open symbols show rejected data.

recognisable geological event may take place over a period longer than the analytical uncertainty on a single date. We therefore have adopted a broader approach, which fits a series of Gaussian curves to the age spectra; the peaks are interpreted as reflecting ‘events’ with durations represented by the full width at half maximum of the peaks.

Trace-element data: derivation of rock type

An extensive study of the trace-element patterns of zircons (Belousova *et al.* 2002) has shown good correlations between these patterns and the chemical composition of the magmatic host rocks. The CART (Classification And Regression Trees) software (Breiman *et al.* 1984) has been applied to U, Th, Y, Yb, Lu and Hf data from this database, to derive a classification tree that can give the parent rock type of a single detrital zircon grain to a specified statistical probability. The classification tree and an analysis of its reliability are given by Belousova *et al.* (2002). Zircons from kimberlites, carbonatites, mafic rocks (dolerites + basalts), syenitic rocks (syenites, larvikites) and Ne-syenites are recognised with a probability of correct classification exceeding 80%. The probability of correct

classification for zircons from granitoids (as distinct from other rock types) is >75%, while the division of granitoids by SiO₂ content is more ambiguous. Zircons from granitoids with 65–70% SiO₂ typically classify as coming from rocks with either higher (40%) or lower (30%) SiO₂ contents. For zircons from the other granite classes, the probability of correct classification by SiO₂ group ranges from 49% for those with 70–75% SiO₂, to 63% for those with >75% SiO₂. Despite this ambiguity, we find that this classification tree provides useful information on the broad composition of the source rocks contributing to a given detrital-zircon sample.

RESULTS

A summary of the data from each sample (Figure 8) presents the probability–density plots of ²⁰⁷Pb/²⁰⁶Pb ages and the Hf-isotope and rock-type data for each grain in each drainage sample. The U–Pb age spectrum of each sample can be compared with that expected from the available data for the rock types mapped in its drainage. This comparison can be used to evaluate the success of our sampling strategy in terms of recognising units and significant events. Unless otherwise noted, the ages assigned to individual units are taken from the work summarised by Page and Sun (1998).

Sample P9686

The drainage samples the Williams Batholith (1530–1500 Ma) and the Mary Kathleen Group (*ca* 1800–1700 Ma). The single large peak in the U–Pb histogram is modelled with Gaussian curves at 1465 ± 36 , 1514 ± 27 and 1566 ± 25 Ma; one grain gives an age of 1766 ± 20 Ma. The zircon sample obviously is dominated by material from the Williams Batholith, with a major age population at *ca* 1514 Ma. The classification of the bulk of the grains as derived from granitoids with 70–75% SiO₂ is consistent with the data of Wyborn (1998), which show that >2/3 of the batholith falls in this SiO₂ range. Younger grains may be derived from rocks affected by late metasomatism (Wyborn 1998). The peak at 1566 Ma is represented mainly by oscillatory zoned grains, but many of these are overprinted by more diffuse zoning; we suggest that these zircons represent an inherited population. The ϵ_{Hf} spectrum shows a single major peak centred on $\epsilon_{\text{Hf}} \approx 0$. The reported age of the Mary Kathleen Group is represented by only one grain; in this area, the unit is dominated by calc-silicate rocks that would have few zircons.

Sample P9687

The drainage samples undifferentiated Soldiers Cap Group (*ca* 1720–1660 Ma), a small area of the Williams Batholith (1500–1530 Ma) and possible Corella Formation (*ca* 1740 Ma) and the Maramungee Granite (*ca* 1544 ± 11 Ma; Page & Sun 1998). The major peak in the U–Pb spectrum can be modelled as three populations at 1471 ± 26 , 1513 ± 17 and 1569 ± 30 Ma, as seen in P9686; the younger two are interpreted as the signal of the Williams Batholith and associated late metasomatic

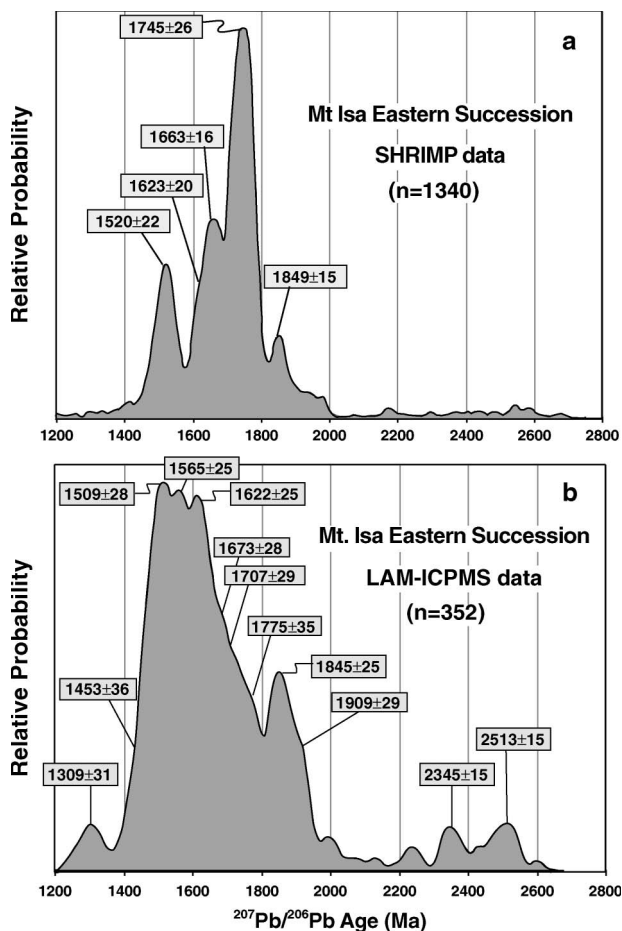


Figure 7 Probability density plots for the SHRIMP U–Pb zircon data (Page & Sun 1998; Ozchron database) and ICPMS data (this study), with peaks modelled as Gaussian forms and uncertainties given by Full Width Half Maximum.

activity (Figure 8). However, in this sample, the 1569 ± 30 Ma peak is dominant; it is defined by magmatic zircons (oscillatory zoning locally overprinted by diffuse zoning), most of which classify as being derived from low-SiO₂ granitic rocks. The age overlaps the poorly defined SHRIMP crystallisation age for the Maramungee Granite; we suggest that similar granites are present in the drainage for sample P9686, and that these older grains are not simply inheritance in the Williams Batholith granites. The higher proportion of low-SiO₂ granitoids may also reflect compositional differences between the older and the younger suite. The range of higher ϵ_{HF} values is defined by zircons from both mafic rocks and silicic granitoids. A small peak at 1667 ± 22 Ma corresponds to one of the age populations expected from the Soldiers Cap Group, while a larger peak at 1744 ± 28 Ma is within the age range proposed for the Leichhardt Superbasin, and may represent the Corella Formation. Other peaks at 1838, 1913 and 1982 Ma probably represent detrital grains from older basement, reworked into Soldiers Cap Group sediments. Single grains with ages > 2000 Ma represent recycled Palaeoproterozoic to Archaean material.

Sample 9688

The drainage samples the Williams Batholith, Soldiers Cap Group, and Doherty Formation (*ca* 1725 Ma). The major peak in the U–Pb spectrum is modelled as two populations at 1510 ± 30 and 1554 ± 35 Ma (dominant). The 1510 Ma group is expected from the Williams Batholith; the 1554 Ma group is similar to that observed in the two previous drainages and suggests the presence of the same group of older granites, either exposed or at depth. These older granitoids contribute most of the grains with $\epsilon_{\text{HF}} > 0$. A peak at 1613 ± 25 Ma is required to fit the spectrum; this is within error of dates from the Tommy Creek Volcanics. A major peak at 1667 ± 22 Ma is similar to an oft-quoted depositional age for the Soldiers Cap Group. Another smaller peak at 1725 ± 16 Ma is consistent with that expected from the Doherty Formation.

Sample 9689

The drainage samples undifferentiated Soldiers Cap Group. No Williams Batholith zircons are present. A major peak at 1630 ± 22 Ma does not correspond to any unit mapped in the drainage but is equivalent to the age of the Tommy Creek Volcanics and the Toole Creek Volcanics; the latter may be present as sills (see below). The dominant peak can be modelled as two populations at 1776 ± 25 Ma and 1831 ± 31 Ma (dominant, and derived largely from mafic rocks). Both may represent inheritance in Soldiers Cap Group rocks. There is a scatter of Palaeoproterozoic to Late Archaean ages; these probably represent inheritance in sediments or volcanics of the Soldiers Cap Group.

Sample 9690

The drainage samples the Llewellyn Creek Formation of the Soldiers Cap Group, some small bodies of granite,

and possible Toole Creek Volcanics (1670–1630 Ma: Page 1988). The major peak, defined by magmatic zircons of granitic derivation, can be modelled with populations at 1520 ± 21 and 1569 ± 23 Ma (dominant), suggesting the presence of both Williams Batholith granites and the older suite correlative with the Maramungee Granite. Most of these zircons have $\epsilon_{\text{HF}} > 0$, unlike those from the Williams Batholith granites (Sample 9685). A small peak at 1460 ± 18 Ma is unidentified, but the grains are near-concordant and may reflect late hydrothermal or magmatic activity. A major peak at 1625 ± 27 Ma is represented largely by zircons from mafic rocks; these are interpreted as the Toole Creek Volcanics (see below). A major peak at 1711 ± 33 Ma may be derived from early Soldiers Cap Group volcanics, while minor peaks at 1856 ± 20 , 1909 ± 22 , 2236 ± 34 and 2433 ± 35 Ma probably represent basement inheritance in the Soldiers Cap Group.

Sample P9691

The drainage samples the Mt Norna Quartzite, Toole Creek Volcanics (1670–1630 Ma) and Llewellyn Formation of the Soldiers Cap Group, as well as several small bodies of granite. The granites are represented by large peaks at 1498 ± 21 Ma (Williams Batholith) and 1555 ± 25 Ma (Maramungee Granite equivalents); the granites obviously contribute disproportionately to the zircon sample, compared to their areal extent in the drainage. The younger of these peaks is strongly skewed to younger ages; a population at 1453 ± 27 is required to fit the spectrum but may not represent a real event. A major peak at 1625 ± 27 Ma consists mainly of zircons from mafic rocks and syenitic ones (differentiates of mafic sills?), and is interpreted as the age of the Toole Creek Volcanics; if this is correct, then the Toole Creek and Tommy Creek volcanic units are temporally equivalent. Many of these grains have an ϵ_{HF} indicating derivation from a depleted mantle source, which would be consistent with a major episode of mafic magmatism. Minor peaks at 1716 ± 22 Ma and 1765 ± 21 Ma probably represent Soldiers Cap Group volcanics and recycled detrital grains from the Llewellyn Formation sediments, respectively, while older minor peaks reflect inheritance in the Soldiers Cap Group.

Sample P9692

The drainage samples the Toole Creek Volcanics (1670–1630 Ma), the Mt Norna Quartzite of the Soldiers Cap Group, Corella Formation (*ca* 1740 Ma), the Gilded Rose Breccia, and many small granite bodies. Relatively few grains were dated successfully. The granites are represented by a peak at 1518 ± 27 Ma, which is a typical Williams Batholith age. The 1550–1570 granites seen in the drainages to the south appear to be absent. The major 1661 ± 36 Ma peak is dominated by grains from syenites (mafic differentiates?). A significant 1778 ± 31 Ma peak and a small peak at 1869 ± 19 Ma may represent recycled grains from the Soldiers Cap Group. The Corella Formation is not obvious in the data, but it is represented in this area by calc-silicate rocks that would not be expected to contribute many zircons.

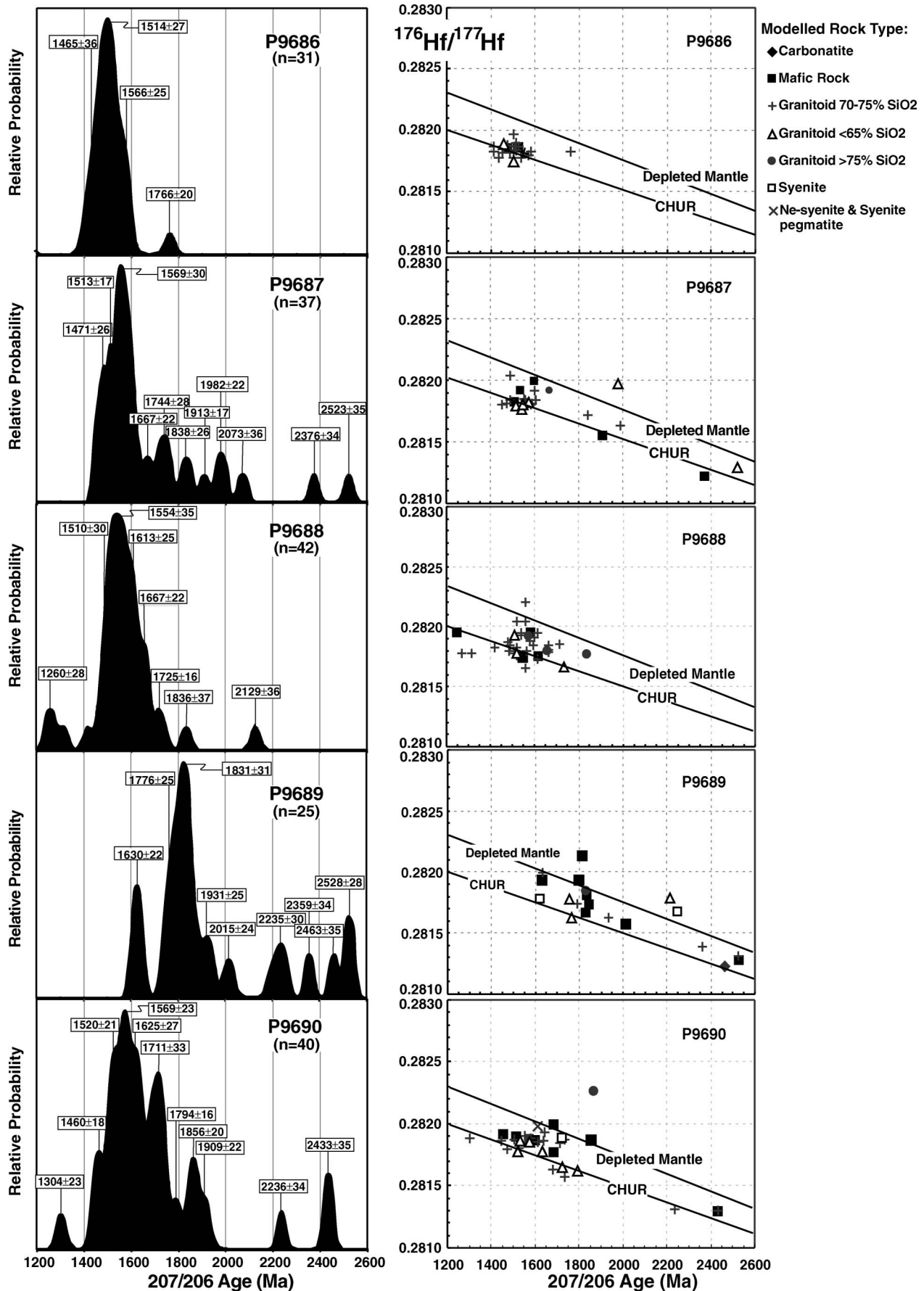


Figure 8 Age, Hf-isotope, and rock-type data for each sample.

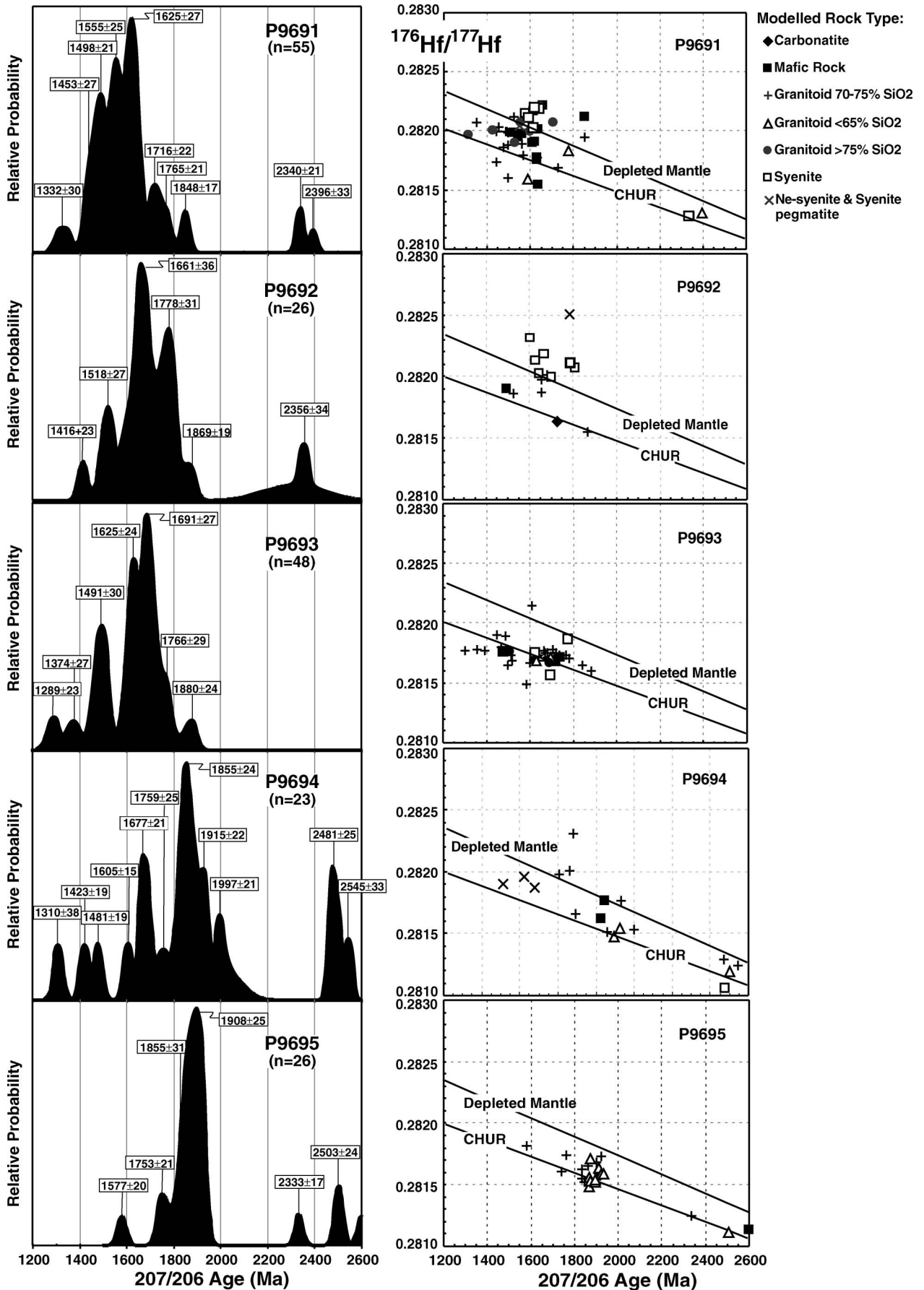


Figure 8 (Continued).

Sample P9693

The drainage samples the Naraku Batholith (*ca* 1500 Ma), the Corella Formation, and rocks mapped as Soldiers Cap Group, but physically separated from the main outcrop area to the south. The large peak at 1491 ± 30 Ma is interpreted as representing the Naraku Batholith; it is somewhat younger than expected, and may be skewed by late-magmatic metasomatic activity (Wyborn 1998). The major peak at 1625 ± 24 Ma is similar to that seen in the Toole Creek Volcanics to the south, and the zircons defining this age include several from mafic to syenitic rocks. However, the $^{176}\text{Hf}/^{177}\text{Hf}$ of these grains is significantly lower than the mean recorded in the zircons interpreted as Toole Creek Volcanics material to the south, and this unmapped unit may be distinct from the Toole Creek Volcanics. The main peak at 1691 ± 27 Ma is consistent with Soldiers Cap Group, and the smaller one at 1766 ± 29 Ma may represent recycled grains in Soldiers Cap Group sedimentary rocks.

Sample P9694

The drainage lies entirely within rocks mapped as possible Soldiers Cap Group. Relatively few grains were successfully dated, and most were too discordant to use. A peak at 1677 ± 21 Ma may represent volcanic rocks in the Soldiers Cap Group. The major peak at 1855 ± 24 Ma, with a shoulder at 1915 ± 22 Ma, may represent inheritance in the Soldiers Cap Group; the same is true of the 2400–2600 Ma grains. If the rocks in this drainage are correlative with the Soldiers Cap Group, the dominance of 1850–1920 Ma ages may indicate that most of the Soldiers Cap Group here consists of metasedimentary rocks. On the other hand, the pattern of ages is similar to that seen in SHRIMP data from a sample of the Double Crossing Metamorphics (Page & Sun 1998) and may indicate the presence of an older unit in this drainage.

Sample P9695

This drainage also is mapped as possible Soldiers Cap Group. A small peak at 1753 ± 21 Ma is within the age span of the Soldiers Cap Group volcanics (Page & Sun 1998). The major peaks are at 1855 ± 31 and 1908 ± 25 Ma, and there are several Palaeoproterozoic or Late Archaean grains. These data suggest that the drainage is dominated either by rocks older than the Leichhardt Superbasin, or by Soldiers Cap Group sedimentary rocks with a very large component of basement-derived zircons. The high proportion of zircons from low-Si granitoids is not typical of other samples from the Soldiers Cap Group.

SUMMARY

The age spectrum, Hf-isotope data, and rock-type data for each sample are grouped in Figure 8. As noted above, there is generally good agreement between the observed age peaks and those expected from a

comparison of the mapped geology and the available SHRIMP data on individual units, especially considering the relatively small number of SHRIMP samples that lie within the drainages sampled here. This overall agreement indicates that the scale of sampling, the selection of zircon grains, and the number of grains analysed were appropriate to the problem of outlining the geological evolution of this terrane.

Some units have not been recognised where expected; these are primarily the Mary Kathleen Group in the south, and the Corella Formation in several drainages. In each case, these formations are dominated by, or inferred from, the presence of calc-silicate units that would not be expected to contribute many zircons. Some units are recognised in the zircon data where they are not mapped in the drainage. These include the Toole Creek Volcanics (large mafic sills), and older, mainly low-SiO₂, granitoids temporally correlative to the Maramungee Granite.

The Toole Creek Volcanics provide distinctive zircons that classify as derived from mafic rocks or their syenitic differentiates; many have a high $^{176}\text{Hf}/^{177}\text{Hf}$ indicating mantle derivation (see samples P9689–P9691). The spread of these grains south of drainage P9691 suggests either stream capture or that the Toole Creek Volcanics are present but have not been recognised during mapping. Our preferred age for this important group of mafic volcanics is *ca* 1625 Ma, suggesting a correlation with the Tommy Creek Volcanics.

The data from drainage P9687, which samples the Maramungee Granite, indicate that the signature of such older granites is an age peak around 1560 ± 30 Ma, with a large proportion of zircons from relatively low-Si granitoids that have $\epsilon_{\text{Hf}} > 0$. This age is found in large numbers of obviously magmatic grains with pronounced oscillatory zoning, and we interpret it as representing a significant igneous event. The same broad age peak (ranging from 1555 ± 25 to 1569 ± 23 Ma in different samples) appears in drainages P9688, P9690 and P9691. This may indicate that these older granites are more widespread than indicated by the mapping, or that they are so voluminous in the crust beneath this area that they contribute a very substantial inheritance to the younger granites. The fact that this age peak is accompanied in each case by a higher relative abundance of zircons from low-Si granitoids favours the presence of these granites in outcrop.

The zircons from the rocks mapped as possible Soldiers Cap Group in the northern two drainages (P9694, P9695) on the Boomarra Horst are dominated by grains older than 1800 Ma, and similar ages appear in many of the other samples. Most of these older zircons have rounded and abraded morphologies (Figure 9), which strongly suggests that they are detrital grains, recycled from the sediments of the Soldiers Cap Group. As noted above, the high abundance of zircons from low-Si granitoids in samples P9694 and P9695 is not typical of detrital material in the classic Soldiers Cap Group to the south, and this suggests some difference in provenance.

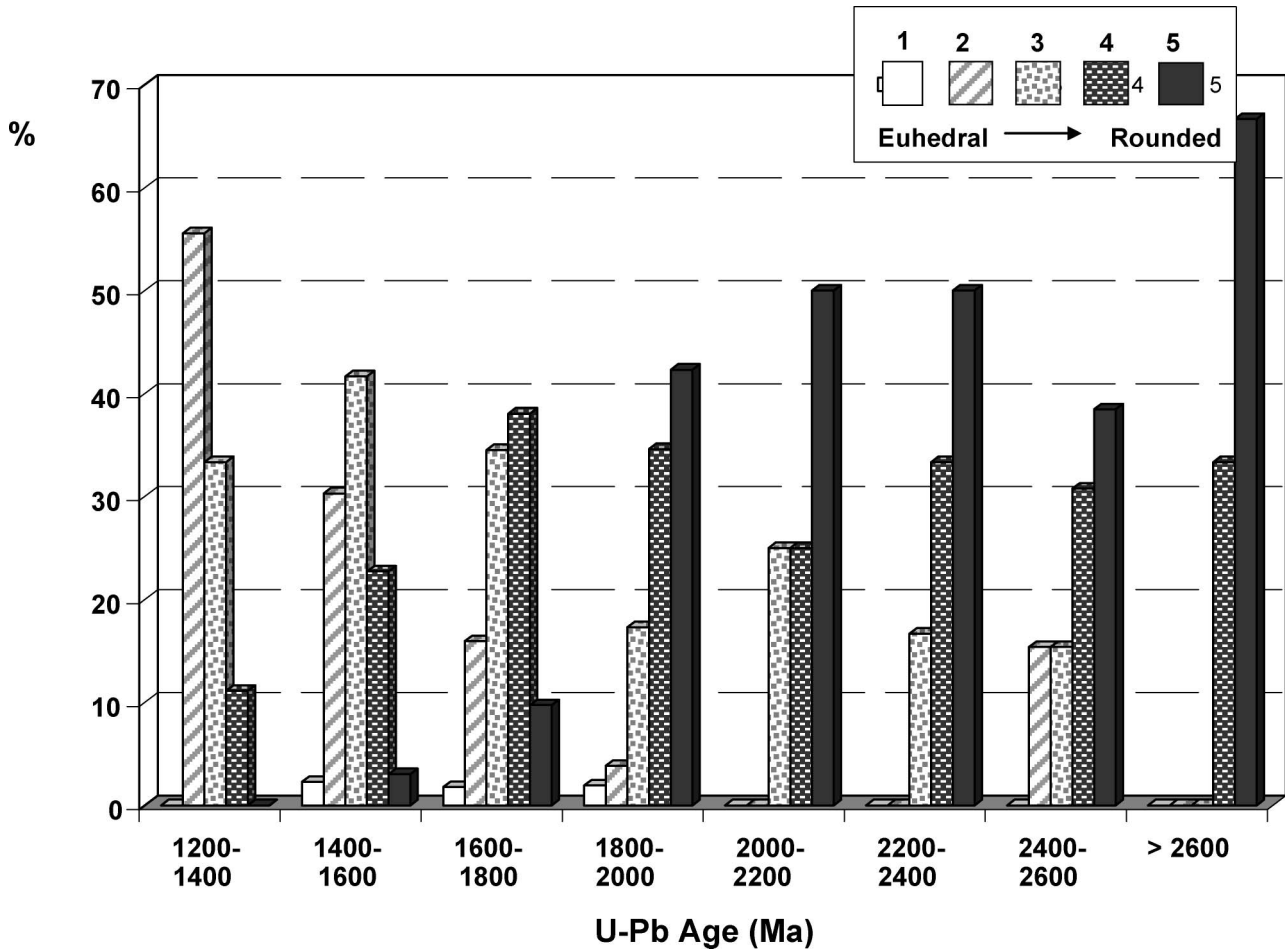


Figure 9 Roundness indices (Appendix 2*) vs UPb age. The greater roundness of grains older than 1.8 Ga suggests that most are recycled grains derived from metasediments of the Soldiers Cap Group.

DISCUSSION

Definition of event ages

The spectrum for SHRIMP data from the Eastern Succession are compared with the age data for the accepted grains from the 10 drainage samples in Figure 7. The SHRIMP data for all previously analysed rock samples from the Eastern Succession can be adequately fitted with only five major peaks: 1520 ± 22 Ma 1623 ± 20 Ma, 1663 ± 16 Ma, 1745 ± 26 Ma and 1849 ± 15 Ma.

The LAM-ICPMS U-Pb data from the present study require 10 Gaussian distributions to provide an adequate fit to the cumulative probability curve. These are (with $\pm 1\sigma$ range) 1309 ± 31 Ma (number of analyses, $n=5$); 1453 ± 36 Ma ($n=29$); 1509 ± 28 Ma ($n=46$); 1566 ± 25 Ma ($n=37$); 1622 ± 25 Ma ($n=43$); 1673 ± 28 Ma ($n=29$); 1707 ± 29 Ma ($n=34$); 1775 ± 35 Ma ($n=15$); 1849 ± 25 Ma ($n=23$); and 1909 ± 28 Ma ($n=15$). We also recognise two small Palaeoproterozoic – Late Archaean populations at 2345 ± 15 Ma ($n=4$) and 2513 ± 14 Ma ($n=5$). The 1509, 1622, 1673, 1775, and 1849 Ma peaks correspond within error with the major peaks seen in the SHRIMP database. The 1566 Ma peak is not strongly represented in the SHRIMP data; we suggest that this reflects

limited sampling of the Maramungee Granite and its correlatives.

Do these age peaks reflect real events? For most of the peaks from 1500 to 1800 Ma, this question can be answered in the affirmative by reference to known magmatic activity in the Eastern Succession. The 1309 Ma peak is not readily identifiable with any dated igneous event. The 1453 Ma peak is a shoulder on the main 1509 Ma peak, which represents the granites of the Williams and Naraku Batholiths, and may reflect late magmatic hydrothermal activity and lead loss rather than a separate event. However, it is a significant peak on its own in some drainages where the 1509 peak is absent or small, and this suggests that it represents a distinct lithology. Wyborn (1998) has reported a 1488 ± 11 Ma K-Ar age for sericite from the widespread quartz-albite bodies in the area, and these metasomatic rocks commonly carry large zircons (L. Wyborn pers. comm. 2000). The 1566 Ma peak is essentially the age of the older granitoids such as the Maramungee Granite but includes other rock types as well. The present data strongly suggest that these older granites are more widespread than previously recognised.

The 1622 Ma peak corresponds to the reported age of the Tommy Creek Volcanics and is dominated by zircons from mafic rocks and their syenitic differentiates; the geographic distribution of zircons with these ages suggest that this also represents the age of the Toole Creek Volcanics, and that these rocks may be more widespread than previously recognised. The 1673 Ma peak is similar to estimates of the depositional age (volcanic rocks) of the Soldiers Cap Group (Page & Sun 1998). The 1707 Ma peak represents a major age population at Cannington and elsewhere in the Soldiers Cap Group. These observations suggest that the identification of age peaks with igneous events, using the 'event simulation' approach, is valid.

The peaks with ages greater than *ca* 1800 Ma probably are sampled here as inherited detrital grains, largely reworked from sediments of the Soldiers Cap Group (or older rocks in the northern part of the area), or brought up as inherited grains in younger volcanic or intrusive rocks. This is consistent with their generally rounded and abraded morphology (Figure 9), whereas there are few rounded zircons with ages < 1800 Ma. However, by analogy with the younger peaks, these older grains are considered to reflect the ages of significant igneous events in the source area of the Soldiers Cap sedimentary rocks, or in the basement of the Eastern Succession. We therefore suggest that the age peaks defined by the LAM-ICPMS U–Pb data represent significant geological events in the evolution of the Eastern Succession.

Correlations within the Soldiers Cap terrane

The data collected here can be used to assess two major questions regarding correlations within the terrane. One is the relative stratigraphic position of the high-grade Fullarton River Group (samples 9687–9689) and the lower-grade Soldiers Cap Group rocks in the Cloncurry area. One model (Page & Sun 1998) regards the two as equivalent, while another (Beardsmore *et al.* 1988) (Figure 3) suggests that the Fullarton River Group underlies the classic Soldiers Cap Group. If the data points related to the Williams Batholith and Maramungee Granites (and correlatives) are stripped out, we find that the youngest ages recorded in the Fullarton River section are 1630 ± 22 Ma (sample P9689) and 1613 ± 25 Ma (P9688); the younger age is defined by a cluster of concordant zircons. These are comparable to the youngest ages in samples P9690 and P9691 (1625 ± 27 Ma), interpreted as the age of the Toole Creek Volcanics and the Tommy Creek Volcanics. If the Toole Creek Volcanics are interpreted as sills, this correspondence in minimum ages does not constrain the relative ages of the Fullarton River Group and the Soldiers Cap Group of the Cloncurry area. However, the presence of age peaks at *ca* 1660–1670 and 1710–1740 in both areas suggests that the Fullarton River Group and the classic Soldiers Cap Group are temporally equivalent. They also share major peaks, with similar Hf-isotope characteristics, at *ca* 1765–1795 Ma and 1830–1870 Ma, suggesting similar provenance.

The samples (P9693–9695) from the possible Soldiers Cap Group of the Boomarra Horst allow a similar

evaluation. P9693 is dominated by zircons with ages of 1625 ± 24 Ma, equivalent to the Tommy Creek Volcanics age, and 1691 ± 27 Ma, suggesting that the rocks in this drainage, like those of the Fullarton River Group to the south, are correlative with the classic Soldiers Cap Group. Samples P9694 and P9695 are dominated by zircons with ages > 1850 Ma, which is older than accepted ages for the deposition of the Soldiers Cap Group. P9694 also contains zircon populations as young as 1605 ± 15 and 1677 ± 21 Ma, indicating that rocks contemporaneous with the Soldiers Cap Group are present in the drainage. Their dominantly rounded morphology (Figure 9) suggests that the older zircons may be clastic grains in Soldiers Cap sediments.

The younger zircons are absent in P9695, which lies 40 km to the north of P9694. This raises the possibility that rocks older than the Soldiers Cap Group are exposed in the northern end of the Boomarra Horst, but this section might also consist of Soldiers Cap Group sedimentary rocks, without volcanic rocks that could constrain the true depositional age. The zircon populations of samples P9694 and P9695 are dominated by rounded and abraded grains (Figure 9; Appendix 2*), suggesting that they are recycled from younger sedimentary rocks rather than outcropping old igneous rocks. We therefore prefer to interpret the Boomarra Horst rocks as correlative with the Soldiers Cap Group. Further detailed mapping and geochronological work will be necessary to resolve this question.

Event signatures

The Hf-isotope and modelled rock-type data for each time slice ('event') defined from the composite age spectrum are summarised in Figure 10. The T_{DM} model ages give a minimum estimate for the age of the source for the host magma of each grain, while the ϵ_{Hf} data give a broad picture of the relative contributions of ancient and juvenile sources to the magmas represented in the time slice.

LATE ARCHAEOAN – PALAEOPROTEROZOIC (2550–2300 Ma)

These inherited grains give a limited picture of the oldest crust in the region. The older group (2513 ± 14 Ma) consists mainly of zircons from low-Si granitoids, while the younger group (2345 ± 15 Ma) contains both high-Si granitoids and mafic/syenitic rocks. The older group contains more juvenile material ($\epsilon_{Hf} = 0$ to $+5$) while the younger group consists mostly of recycled material ($\epsilon_{Hf} < 5$). T_{DM} model ages for the older group are only 200–400 million years older than crystallisation ages, indicating a significant period of crustal growth in the Late Archaean. Similar model ages are found for the younger group, indicating reworking of the Late Archaean crust to produce Palaeoproterozoic magmatic rocks.

1940–1880 Ma

This period is represented by an abundance of both low-Si and high-Si granitoids, with minor input of mafic rocks. ϵ_{Hf} values cluster from -5 to $+5$, indicating that most of these rocks were derived by reworking of

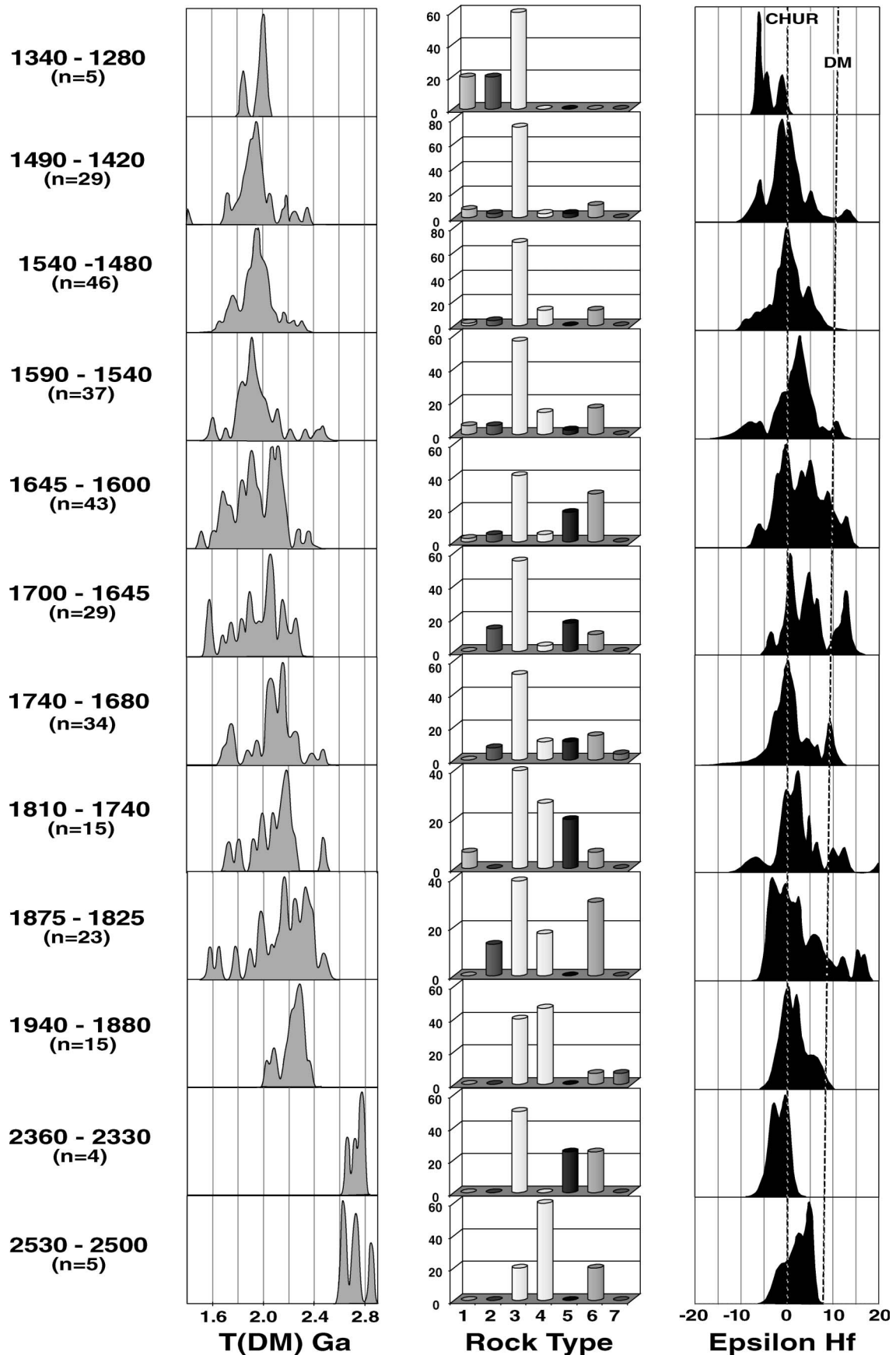


Figure 10 Hf-isotope and rock-type data for time slices derived from age peaks (Figure 7b). Rock types: 1, nepheline–syenite and syenite pegmatites; 2, granitoid > 75% SiO₂; 3, granitoid 70–75% SiO₂; 4, granitoid < 65% SiO₂; 5, syenite; 6, mafic rocks; 7, carbonatites/alkaline rocks.

pre-existing crust. T_{DM} model ages define a narrower range than in most time slices, peaking at 2400–2200 Ma. These are minimum ages for the source rocks.

1875–1825 Ma

This time slice, which overlaps with the Barramundi Orogeny (1900–1870 Ma) in the Western Succession and Kalkadoon–Leichhardt Belt, shows a greater relative abundance of high-Si and very high-Si granitoids than the 1940–1880 Ma period, but there is also a greater input of mafic rocks. These mafic rocks contribute to the higher mean ϵ_{HF} values, and a spread toward lower T_{DM} compared with the 1909 \pm 29 Ma event. The peak of T_{DM} ages from 2200 to 2400 Ma indicates that the Late Archaean crust was still being remelted during the 1849 \pm 50 Ma event, but juvenile input was more important than in the previous time slice.

1810–1740 Ma

This time slice shows a rock-type distribution similar to the previous one. The juvenile contribution is smaller, with ϵ_{HF} values clustering about zero (-5 to $+5$). T_{DM} values cluster between 2000 and 2200 Ma, and the major peak at 2200–2400 Ma that characterised the two earlier time slices has largely disappeared. This event therefore appears to have involved mainly reworking of older crust, but a significant component sampled during the 1909 Ma and 1849 Ma events is no longer well represented. This time slice includes the eruption of significant volumes of continental tholeiites across the region around 1780 Ma (Betts *et al.* 1988), but this event probably is recorded weakly, if at all, in the zircon data, because of the paucity of zircons in tholeiitic lavas.

1740–1680 Ma

This time slice is dominated by high-Si granitoids, and the ϵ_{HF} data indicate a juvenile contribution only slightly higher than in the previous time slice. The T_{DM} data show a major peak between 2000 and 2200 Ma, suggesting that most of these granitoids were derived from Palaeoproterozoic crust; the 2200–2400 Ma model ages seen in the pre-Barramundi time slices are essentially absent.

1700–1645 Ma

Compared with the previous time slice, this event shows a larger input of mafic rocks (mafic/syenitic zircons), and the Hf-isotope data show that this mafic input is derived largely from juvenile mantle sources. T_{DM} ages indicate that the 2000–2200 Ma crustal component was still being tapped to provide granitic rocks (including high-Si granitoids).

1650–1600 Ma

The rock-type distribution in this time slice is very similar to that in the previous one, but the proportion of juvenile input from the mantle is significantly higher, as shown by the shift to higher mean ϵ_{HF} values. A large

peak of T_{DM} values from 1800 to 2000 Ma suggests mixing between mantle-derived magmas and crustal material with T_{DM} of 2000–2200 Ma. This time slice includes the Toole Creek and Tommy Creek Volcanics, and the emplacement of thick mafic sills (now amphibolites) is consistent with a large juvenile contribution to the crust.

1590–1540 Ma

This time slice follows a major high-grade metamorphic event (M1) in the Eastern Succession (1584 \pm 17 Ma: Page & Sun 1998; Hand & Rubatto 2002), but pre-dates the main M2 event of the Isan Orogeny at *ca* 1530 Ma (Connors & Page 1995). It includes the intrusion of the older granite suite represented by the Maramungee Granite. The proportion of mafic rocks is lower than in the two previous time slices, and some highly evolved rocks appear (very high-Si granitoids, nepheline syenites, pegmatites). There also is a significant drop in the input of juvenile material, reflected in lower mean ϵ_{HF} . The T_{DM} ages cluster around 1800–2000 Ma, and the 2000–2200 Ma peak that dominated the earlier post-Barramundi time slices is greatly reduced.

1540–1480 Ma

This time slice includes the intrusion of the Williams and Naraku Batholiths, and associated hydrothermal alteration. The samples are dominated by high-Si granitoids, with some more evolved rocks and essentially no mafic input. The peak around $\epsilon_{HF}=0$ indicates that most rocks were derived by reworking of older crust. The T_{DM} data suggest that the dominant source material for these granitoids is the crust generated during the 1673–1622 Ma events.

1490–1420 Ma

This time slice may include intrusive rocks that have not been sampled in earlier dating programs, but the ages also may represent rocks of 1509 \pm 28 Ma age that underwent lead loss soon after intrusion, as a result of hydrothermal activity. It should be stressed that these U–Pb ages do not refer to rims of grains, but appear to represent the ages of zircon cores, and many of the ages are concordant. The ϵ_{HF} data are similar to those for the 1509 \pm 28 Ma granitoids, as is the T_{DM} peak near 1900 Ma.

1340–1280 Ma

The rock types included in this time slice are high-Si to more evolved granitoids. It is not clear whether they represent previously unrecognised, younger intrusive rocks, or aberrant dates related to early lead loss in older rocks. Their T_{DM} distribution peaks around 2000 Ma, but there are too few data to establish whether this is significantly different from the rocks in the two earlier time slices.

Crustal evolution in the Eastern Succession

The data for the time slices described above allow the history of crustal evolution (as distinct from the

structural history) of the Eastern Succession to be divided into three main stages, or four if the Palaeoproterozoic – Late Archaean history is included (Figure 11). In each stage, magmatic rocks have been produced by remelting of pre-existing crust, and there are also varying proportions of juvenile rocks derived from the depleted mantle. The end of each stage is marked by a distinct change in the composition and mean age of the crust available for recycling.

STAGE 1: PALAEOPROTEROZOIC – LATE ARCHAEOAN

The Late Archaean zircons have T_{DM} ages close to their U–Pb ages, indicating a period of significant crustal generation. The few analysed zircon grains are derived from low-Si granitoids and mafic rocks, suggesting a TTG (tonalite–trondhjemite–granodiorite)-type crust. During the subsequent Palaeoproterozoic period, the few available data suggest reworking of this Late Archaean Crust, with little net crustal growth.

STAGE 2: 1940–1825 Ma

This stage opens with a major episode of crustal reworking (1940–1880 Ma), with little clear evidence for juvenile input. The T_{DM} age of the reworked material is 2200–2400 Ma. Modelling of the Hf-isotope data (Figure 12) indicates that this reworked material could be derived from a Late Archaean (*ca* 2.5 Ga) crust, represented by the 2300–2600 Ma zircons from this study, if this crustal source had a mean $^{176}\text{Lu}/^{177}\text{Hf} = 0.022$. This is higher than the mean crustal value of 0.015 (Griffin *et al.* 2004); it indicates a crust somewhat more mafic than the mean continental composition and is consistent with a TTG-type crust.

Reworking of this Palaeoproterozoic/Late Archaean crust continued into the latter part of this stage (1875–1825 Ma). This period overlaps with that of the Barramundi Orogeny (1900–1870 Ma) recognised in the Western Succession and the Kalkadoon–Leichhardt Belt (Figure 2), and the intrusion of the Kalkadoon Batholith (1860–1850 Ma). Crustal reworking produced rocks with T_{DM} model ages of 2200–2400 Ma; this was accompanied by a significant mantle input, represented by mafic rocks with ϵ_{Hf} from +5 to +15. A large peak of T_{DM} ages between 1900 and 2200 Ma probably reflects mixing between these two sources. This could occur by remelting, on a short time-scale, of lower crust comprising a physical mixture of the older crust with younger mantle-derived intrusions, and/or by mixing of magmas from the two sources. Such mixing of magmas, while still a matter of debate, has been documented by detailed studies of Hf isotopes in zircons from I-type igneous complexes (Griffin *et al.* 2002). The abundance of juvenile mafic material suggests that rifting may have been important during this stage.

STAGE 3: 1810–1600 Ma

The beginning of this stage is marked by the reduced importance of the crustal source with $T_{DM} = 2200$ –2400 Ma. During the 1810–1740 Ma period, the T_{DM} model age of the oldest crust contributing to the

production of igneous rocks shifts toward 2000–2200 Ma, corresponding to the mixed signature developed near the end of the previous stage. This source continues to make a major contribution to the igneous rocks erupted throughout Stage 3.

The proportion of juvenile input is relatively low early in this stage but increases as time goes on, suggesting that crustal extension became more important. The Leichhardt Rift Event (1780–1755 Ma) in the western part of the Mt Isa Inlier coincides with the first event in this stage. The major Mt Isa Rift Event (Betts *et al.* 1998; Giles *et al.* 2002, 2004) extends from 1708 to 1595 Ma, representing the rest of Stage 3. The degree of mixing between crust and juvenile mantle sources also increases with time from 1700 to 1600 Ma, producing a large peak of T_{DM} ages from 1800 to 2000 Ma. This stage ends, like the previous one, with a homogenisation event, reflected in a major reduction in the contribution from the oldest crustal source ($T_{DM} = 2000$ –2200 Ma). This homogenisation coincides with the beginning of the Isan Orogeny.

Stage 3 includes the development of the three super-basins discussed above (Leichhardt, 1790–1730 Ma; Calvert, 1730–1670 Ma; Isa, 1670–1590 Ma). The detrital-zircon data primarily reflect magmatic episodes, with a probable bias toward more felsic ones, and provide only a broad picture of this tectonic–stratigraphic development. The 1810–1740 Ma time slice corresponds roughly to the development of the Leichhardt Superbasin. There is no obvious break corresponding to the change from the Calvert Superbasin to the Isa Superbasin, but as noted above, the hiatus between the two basins is not observed in the Eastern Succession. The zircon data show a greater juvenile input after *ca* 1700 Ma, suggesting a more active extension, which may be associated with the change in tectonic style from the Calvert Superbasin to the Isa Superbasin.

STAGE 4: AFTER 1600 Ma

This stage is dominated by the intrusion of granitoids, beginning with an older (1566 ± 25 Ma) suite that includes the Maramungee Granite, and continuing into the major magmatic period of the Williams and Naraku Batholiths. These I-type granitoids can be modelled as derived almost entirely from the mixed crustal source that developed during the latter half of the previous orogenic stage. However, a scatter of T_{DM} ages > 2000 Ma shows that the older sources were still contributing to magmatism. A minor input of juvenile material may be reflected in some T_{DM} ages < 1800 Ma, but this requires a mixing between crust and mantle sources; there is little evidence in the zircon data for the eruption of juvenile magmas at the present level of exposure.

SUMMARY

These data suggest that the two post-Archaean tectonic cycles recognised in the zircon data (Stages 2 and 3) each started with the generation of intracrustal magmas and progressed to a greater degree of juvenile input; this sequence may reflect progressive crustal extension as documented in several syntheses of the geological

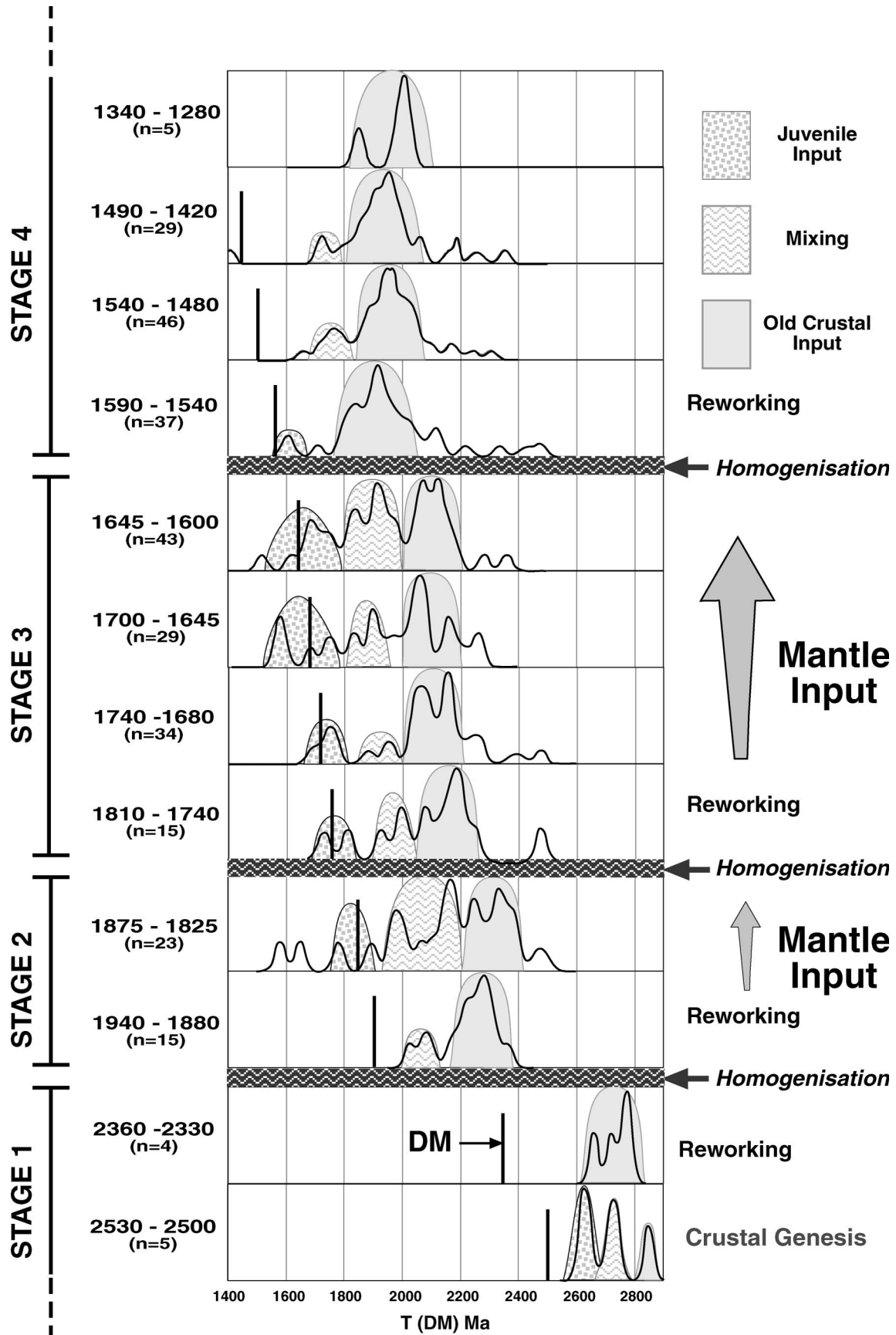


Figure 11 Summary of the crustal evolution of the Eastern Succession. Shading of peaks in the T_{DM} data identifies major groups derived from reworked crust and from juvenile (mantle) sources [note changing composition of the Depleted Mantle (DM) with time], intermediate values probably reflect mixing of material from these two sources.

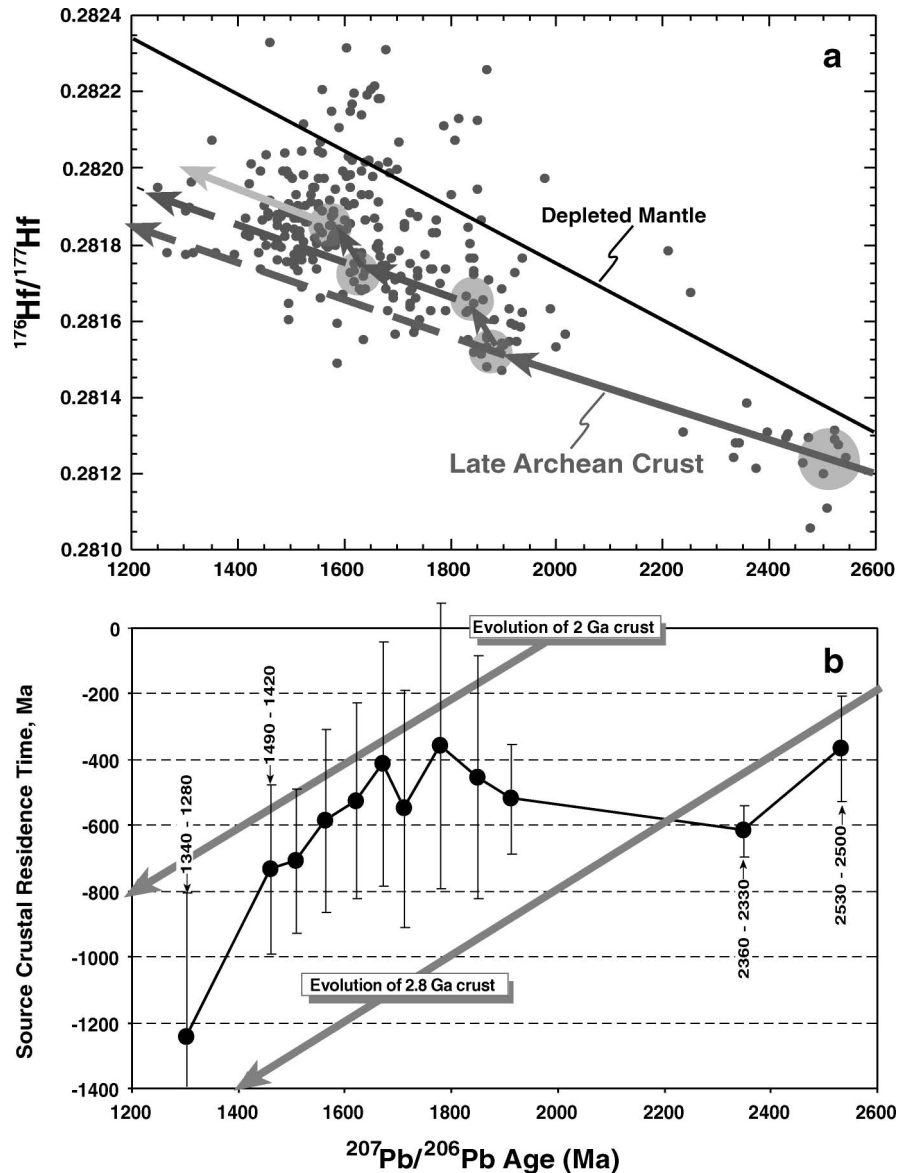


Figure 12 (a) Age vs Hf-isotope composition for all zircons. The model curves illustrate the progressive mixing of juvenile material into the older crust and the homogenisation of this mixed crust to produce the major crustal source for the next stage of evolution, as shown in Figure 11. (b) Event Signature curve for the Eastern Succession; mean magma source residence time ($\text{Age} - T_{\text{DM}}$) is plotted against time. Juvenile material was added to the crust from 1.9 to 1.8 Ga, and this crust was reworked until ca 1.7 Ga; a new juvenile input followed to ca 1.6 Ga, but after that time, magma production was dominated by reworking of crustal material.

evolution of the Inlier (Betts *et al.* 1998, 2006; McLaren & Sandiford 2001; Giles *et al.* 2002, 2004). As this juvenile input increased, so did the degree of mixing between sources, resulting in a composite crust. This mixing might represent the intrusion of mantle-derived magmas into older continental crust, followed on a short time-scale by remelting due to generally rising geotherms.

Each cycle closed with an apparent homogenisation of the crustal source(s), which we interpret as the geochemical consequence of physical mixing processes in the crust. These processes might include extension and recompression, concentrated in mid- to lower crustal levels weakened by heating (McLaren & Sandiford 2001). As a result of such homogenisation, the mean isotopic composition of the recycled component in the igneous rocks derived by crustal melting at the beginning of the next stage is shifted noticeably toward more juvenile values. The generation of the post-1600 Ma I-type granitoids involved little obvious

juvenile input, and melting may have depended on intracrustal heat sources (McLaren *et al.* 1999).

Correlations with other Mt Isa 'terrane's'

The crustal history derived from the Soldiers Cap Group zircon populations is very similar in many respects to that established for the Western Succession and the Kalkadoon–Leichhardt Belt (Figure 2). The 1940–1880 event correlates with the Yaringa Metamorphics (1890 Ma), and the 1875–1825 event includes the ages of both the Kurbayia Migmatite (1860–1850 Ma) and the Leichhardt Volcanics (ca 1865 Ma). The period of the Barramundi Orogeny (1900–1870) lies within the first events of Stage 2. The events defined in Stage 3 (1810–1600 Ma) can be correlated with various ages from the superbasin sequences in the Western Succession and the central Kalkadoon–Leichhardt Belt, including the intrusion of the Sybella and Wonga Batholiths. These similarities suggest that the Soldiers Cap Group, while

perhaps allochthonous, shares much of its crustal history with the rest of the Mt Isa Block and is unlikely to be transported far. A more detailed comparison of crustal evolution histories across the different parts of the block must await the generation of comparable volumes of Hf-isotope (or Nd-isotope) data from the Western Succession and the Kalkadoon–Leichhardt Belt.

ARCHAEOAN CRUST BENEATH THE EASTERN SUCCESSION

Small numbers of Archaean zircons are present in Proterozoic sedimentary and igneous rocks throughout northern Australia (Page 1988; Page & Sun 1998; Page & Sweet 1998) and have been interpreted as inherited or recycled grains, rather than indication of a local Archaean basement. However, the present study has identified many young (< 1600 Ma) zircons with low $^{176}\text{Hf}/^{177}\text{Hf}$ (0.2815–0.2816, $\epsilon_{\text{HF}} = -5$ to -10). Their presence strongly suggests that Late Archaean crust was still present beneath the Eastern Succession in Mesoproterozoic time and contributed to the production of felsic magmas up to and through Stage 4. In a simple model (Figure 12), Late Archaean crust is defined by the Hf-isotope composition of the 2.3–2.6 Ga zircons in our samples. If this crust has a mean $^{176}\text{Lu}/^{177}\text{Hf}$ of 0.02–0.022 (a mafic to intermediate bulk composition), its T_{DM} age is *ca.* 2.9 Ga. As it evolves, it can provide the least radiogenic magmas observed through the entire Proterozoic history of the Eastern Succession. If an average crustal composition ($^{176}\text{Lu}/^{177}\text{Hf} \approx 0.015$) is assumed, the source would have a Depleted Mantle age as low as 2.6 Ga, which also is consistent with the ages of the oldest observed zircons in our samples. If a Proterozoic crustal source is proposed for the lowest $^{176}\text{Hf}/^{177}\text{Hf}$ magmas produced from 1800 to 1500 Ma, two improbable constraints are imposed: it would need to have a highly felsic composition ($^{176}\text{Lu}/^{177}\text{Hf} \ll 0.015$) and it could not contribute inherited zircons to later magmatism.

In the model shown in Figure 12, the Late Archaean crustal source evolved until *ca.* 1.9 Ga, when it was partially melted to provide granitic rocks with a mean $^{176}\text{Hf}/^{177}\text{Hf} = 0.28155$ (Figure 12a). Further remelting of this source occurred during the 1845–1840 Ma event, during which it was mixed with more juvenile material and partially homogenised to produce a composite source with a mean $^{176}\text{Hf}/^{177}\text{Hf} = 0.2817$. This new source material evolved with a mean $^{176}\text{Lu}/^{177}\text{Hf} \approx 0.015$ (Figure 12a); it was again progressively mixed with more juvenile material over the period 1700–1600 Ma, to produce a second composite source material that provided much of the Williams and Naraku Batholiths from *ca.* 1530 to 1450 Ma. Despite this extensive history, the Late Archaean source apparently was still able to contribute to the granitoids of the Williams and Naraku Batholiths, as indicated by 1500 Ma zircons with $^{176}\text{Hf}/^{177}\text{Hf} < 0.2818$.

An alternative model would explain the evolution of the major crustal source toward more isotopically juvenile compositions not by progressive mixing between crustal and mantle sources, but by a progressive change in the composition of the mid- to lower crust

throughout the mid-Proterozoic evolution of the Mt Isa Inlier, due to repeated melt extraction. McLaren and Sandiford (2001) have argued that the concentration of radioelements (K, U, Th) to progressively higher levels of the crust has been responsible for the episodic weakening of the mid- to lower crust, which in turn has allowed episodic deformation and melting, culminating in the production of the late high-level granites through crustal melting. These processes also would affect the mean Lu/Hf of the lower and middle crust. Assuming that melting took place in the stability field of garnet-bearing granulites, each episode of melt removal would tend to increase the mean Lu/Hf of the residue, which would then evolve toward higher $^{176}\text{Hf}/^{177}\text{Hf}$ over time than the less-depleted parts of the crust. Granitoid melts produced at each stage would inherit the $^{176}\text{Hf}/^{177}\text{Hf}$ of their source, but a low Lu/Hf, and their $^{176}\text{Hf}/^{177}\text{Hf}$ would change less rapidly with time. Remelting of these older granitoids would tend to perpetuate the signature of older rocks during the generation of younger magmas.

Figure 12b plots the mean crustal residence time of the magma sources involved at each stage of the area's evolution, given by (U/Pb age – T_{DM}), against time. In this plot, reworking of older crust will produce a downward trend with decreasing age, while juvenile inputs (leading to a lower mean source age) will produce rising trends with decreasing age. This “Event Signature” curve illustrates the increasing degree of juvenile input to the crust from *ca.* 1.9 to 1.8 Ga, a period of reworking until at least 1.7 Ga, and renewed juvenile input to *ca.* 1.6 Ga. After 1600 Ma, the bulk of magmatic rocks were produced largely by reworking of older crust. This event signature curve provides a graphical summary of crustal evolution in the Eastern Succession that can be compared with similar signatures from other terranes to evaluate broad correlations in crustal history.

CONCLUSIONS

1. The LAM-ICPMS analysis of detrital zircon populations from 10 selected drainages has provided an expanded geochronological framework for the Mt Isa Eastern Succession. This framework corresponds in many respects to that derived from earlier U–Pb work on individual rock samples but provides additional information, in particular regarding the distribution and abundance of granitoids older than the Williams and Naraku Batholiths, and of the Toole Creek Volcanics.

2. The presence of abundant inherited zircons in sediments and igneous rocks of the Soldiers Cap Group and younger granitoids allows reconstruction of a crustal history extending back to Late Archaean time, despite the fact that these older units apparently do not appear as outcrop in the sampled areas.

3. Integration of the Hf-isotope and trace-element data with the age spectra provides a detailed event signature for the Eastern Succession. Four major stages of crustal evolution can be recognised in the area: 2500–2330 Ma, 1940–1825 Ma, 1810–1600 Ma and 1590–1420 Ma. Each stage has a distinct pattern of crustal

recycling and juvenile mantle input, and each stage, except the last, ends with a period of crustal homogenisation that is reflected in the isotopic composition of magmatic rocks generated by crustal reworking in the succeeding stage.

4. Crust generated in Late Archaean time was reworked to produce felsic magmas during Palaeoproterozoic time (2360–2330 Ma). Within each of the next two stages, the importance of juvenile crustal generation, relative to reworking of older crust, increased with time, as did the degree of mixing between older crust and juvenile material. At the start of each succeeding stage, this mixed source provided most of the observed magmatic rocks. This pattern suggests that Stages 2 and 3 each reflect increasing crustal extension through time, followed by orogenesis involving the physical mixing of crustal reservoirs.

5. The post-1600 Ma magmatism in the Eastern Succession is dominated by granitoids derived from the mixed crustal reservoir produced in the 1800–1600 Ma stage, with minor input from the *ca* 1850 Ma and Late Archaean reservoirs. There is little evidence of juvenile (mantle-derived) contribution to the crust after 1600 Ma. This raises questions about the source of the heat that produced the major crustal melting responsible for the Williams and Naraku Batholiths (*ca* 1500 Ma).

6. A history of protracted superimposed rifting, with juvenile additions followed by homogenisation, is a distinctive pattern of crustal evolution that, in the case of the Mt Isa Inlier, is linked to world-class metal endowment involving a range of metallogenic styles. This observation can be used as a time-slice template to identify directly comparable events in other terranes or as an “Event Signature” to recognise analogous crustal evolution histories.

7. The extended history evident in samples largely sourced from the outcropping Soldiers Cap Group suggests that the Soldiers Cap ‘terranes’ has shared a comparable crustal evolution history with other sequences in the Mt Isa Inlier. This would imply that although the Soldiers Cap terrane may be thrust over other sequences, it is not grossly allochthonous in terms of shared crustal evolution. A comparative study of event signatures in the Western Succession would be required for a more detailed analysis.

8. The integrated analysis of U–Pb age, Hf-isotope composition, and trace-element patterns in detrital zircons (*TerraneChron*) is a powerful and relatively inexpensive tool for the analysis of terrane-scale crustal evolution, and for the correlation of terranes.

ACKNOWLEDGEMENTS

This study was funded by a Macquarie University Collaborative Research Grant sponsored by BHP Exploration Inc. We are grateful for their input to the project planning and design. We also thank Norm Pearson, Simon Jackson, Carol Lawson and Ashwini Sharma, for their continuous and generally patient assistance with the analytical work, and Geoff Hansen and Jeff Davis for the mineral separations.

The manuscript was significantly enhanced by thoughtful reviews from David Giles, Gordon Lister and Peter Betts. This is contribution 385 from the ARC National Key Centre for Geochemical Evolution and Metallogeny of Continents (<www.els.mq.edu.au/GEMOC>).

REFERENCES

- ANDERSEN T., GRIFFIN W. L. & PEARSON N. J. 2002. Crustal evolution in the SW part of the Baltic Shield. The Hf isotope evidence. *Journal of Petrology* **43**, 1725–1747.
- BEARDSMORE T. J., NEWBERRY S. P. & LAING W. P. 1988. The Maronan Supergroup: an inferred early volcanosedimentary rift sequence in the Mount Isa Inlier, and its implications for ensialic rifting in the Middle Proterozoic of northwest Queensland. *Precambrian Research* **40/41**, 487–507.
- BELOUSOVA E. A., GRIFFIN W. L., SHEE S. R., JACKSON S. E. & O'REILLY S. Y. 2001. Two age populations of zircons from the Timber Creek Kimberlites, Northern Territory, as determined by laser-ablation ICPMS. *Australian Journal of Earth Sciences* **48**, 757–765.
- BELOUSOVA E. A., WALTERS S., GRIFFIN W. L., O'REILLY S. Y. & FISHER N. I. 2002. Zircon trace-element compositions as indicators of source rock type. *Contributions to Mineralogy and Petrology* **143**, 602–622.
- BENNETT V. C., NUTMAN A. P. & MCCULLOCH M. T. 1993. Nd isotopic evidence for transient, highly depleted mantle reservoirs in the early history of the Earth. *Earth and Planetary Science Letters* **119**, 299–317.
- BETTS P. G., GILES D., MARK G., LISTER G. S., GOLEBY B. R. & AILLÈRES L. 2006. Synthesis of the Proterozoic evolution of the Mt Isa Inlier. *Australian Journal of Earth Sciences* **53**, 187–211.
- BETTS P. G., LISTER G. S. & O'DEA M. G. 1998. Asymmetric extension of the Middle Proterozoic lithosphere, Mount Isa terrane, Queensland, Australia. *Tectonophysics* **296**, 293–316.
- BIZZARRO M., BAKER J. A., HAACK H., ULFBECK D. & ROSING M. 2003. Early history of Earth's crust–mantle system inferred from hafnium isotopes in chondrites. *Nature* **421**, 931–933.
- BLACK L. P. & GULSON B. L. 1978. The age of the Mud Tank carbonatite, Strangways Range, Northern Territory. *BMR Journal of Australian Geology & Geophysics* **3**, 227–232.
- BLAKE D. H. 1987. Geology of the Mount Isa Inlier and environs, Queensland and Northern Territory. *Bureau of Mineral Resources Bulletin* **225**.
- BLAKE D. H. & STEWART A. J. 1992. Stratigraphy and tectonic framework, Mount Isa Inlier. In: Stewart A. J. & Blake D. H. eds. *Detailed Studies of the Mount Isa Inlier*, pp. 1–11. Australian Geological Survey Organisation Bulletin **243**.
- BLICHERT-TOFT J. & ALBARÈDE F. 1997. The Lu–Hf geochemistry of chondrites and the evolution of the mantle–crust system. *Earth and Planetary Science Letters* **148**, 243–258 [Erratum 154 (1998), 349].
- BLICHERT-TOFT J., ALBARÈDE F., ROSING M., FREI R. & BRIDGWATER D. 1999. The Nd and Hf isotopic evolution of the mantle through the Archean. *Geochimica et Cosmochimica Acta* **63**, 3901–3914.
- BREIMAN L., FRIEDMAN J. H., OLSHEN R. A. & STONE C. J. 1984. *Classification and Regression Trees*. Wadsworth International, Belmont, CA.
- CONNORS K. A. & PAGE R. W. 1995. Relationships between magmatism, metamorphism and deformation in the western Mount Isa Inlier, Australia. *Precambrian Research* **71**, 131–153.
- DEBIEVRE P. & TAYLOR P. O. P. 1993. Table of the isotopic composition of the elements. *International Journal of Mass Spectrometry. Ion Processes* **123**, 149.
- DERRICK G. M., WILSON I. H. & HILL R. M. 1976. Revision of stratigraphic nomenclature in the Precambrian of northwestern Queensland, 5 Soldiers Cap Group. *Queensland Government Mining Journal* **77**, 601–604.
- GILES D. & NUTMAN A. P. 2002. SHRIMP U–Pb monazite dating of a *ca* 1590 amphibolite facies metamorphism in the eastern Mt Isa Inlier. *Australian Journal of Earth Sciences* **49**, 455–465.

- GILES D. & NUTMAN A. P. 2003. SHRIMP U–Pb dating of the host rocks of the Cannington Ag–Pb–Zn deposit, southeastern Mt Isa Block, Australia. *Australian Journal of Earth Sciences* **50**, 295–309.
- GILES D., BETTS P. & LISTER G. 2002. Far-field continental backarc setting for the 1.80–1.67 basins of northeastern Australia. *Geology* **30**, 823–826.
- GILES D., BETTS P. & LISTER G. 2004. 1.8–1.5 Ga links between the North and South Australian Cratons and the Early–Middle Proterozoic configuration of Australia. *Tectonophysics* **380**, 27–41.
- GRIFFIN W. L., BELOUSOVA E. A., SHEE S. R., PEARSON N. J. & O'REILLY S. Y. 2004. Archean crustal evolution in the northern Yilgarn Craton: U–Pb and Hf-isotope evidence from detrital zircons. *Precambrian Research* **131**, 231–282.
- GRIFFIN W. L., PEARSON N. J., BELOUSOVA E. A., JACKSON S. R., VAN ACHTERBERGH E., O'REILLY S. Y. & SHEE S. R. 2000. The Hf isotope composition of cratonic mantle: LAM-MC-ICPMS analysis of zircon megacrysts in kimberlites. *Geochimica et Cosmochimica Acta* **64**, 133–147.
- GRIFFIN W. L., WANG X., JACKSON S. E., PEARSON N. J., O'REILLY S. Y., XU X. & ZHOU X. 2002. Zircon chemistry and magma genesis, SE China: *in-situ* analysis of Hf isotopes, Pingtan and Tonglu igneous complexes. *Lithos* **61**, 237–269.
- HAND M. & RUBATTO D. 2002. The scale of the thermal problem in the Mount Isa Inlier. *Geological Society of Australia Abstracts* **67**, 173.
- HORN I., RUDNICK R. L. & McDONOUGH W. F. 2000. Precise elemental and isotope ratio determination by simultaneous solution nebulization and laser ablation-ICP-MS: application to U–Pb geochronology. *Chemical Geology* **164**, 281–301.
- JACKSON S. E., PEARSON N. J., GRIFFIN W. L. & BELOUSOVA E. A. 2004. The application of laser ablation microprobe-inductively coupled plasma-mass spectrometry (LAM-ICP-MS) to *in situ* U–Pb zircon geochronology. *Chemical Geology* **211**, 47–69.
- KETCHUM J. W. F., JACKSON S. E., CULSHAW N. G. & BARR S. M. 2001. Depositional and tectonic setting of the Paleoproterozoic Lower Aillik Group, Makkovik Province, Canada: evolution of a passive margin-foredeep sequence based on petrochemistry and U–Pb (TIMS and LAM-ICP-MS) geochronology. *Precambrian Research* **105**, 331–356.
- KNUDSEN T.-L., GRIFFIN W. L., HARTZ E. H., ANDERSEN A. & JACKSON S. E. 2001. *In situ* hafnium and lead isotope analyses of detrital zircons from the Devonian sedimentary basin of NE Greenland: a record of repeated crustal reworking. *Contributions to Mineralogy and Petrology* **141**, 83–94.
- LUDWIG K. R. 2000. Isoplot/Ex version 2.3. A geochronological toolkit for Microsoft Excel. *Berkeley Geochronology Center Special Publication* **1a**.
- MACHADO N. & GAUTHIER G. 1996. Determination of $^{207}\text{Pb}/^{206}\text{Pb}$ ages on zircon and monazite by laser-ablation ICPMS and application to a study of sedimentary provenance and metamorphism in southeastern Brazil. *Geochimica et Cosmochimica Acta* **60**, 5063–5073.
- McLAREN S. & SANDIFORD M. 2001. Long-term thermal consequences of tectonic activity at Mount Isa, Australia: implications for polyphase tectonism in the Proterozoic. In: Miller J. A., Holdsworth R. E., Buick I. S. & Hand M. eds. *Continental Reactivation and Reworking*, pp. 219–236. Geological Society of London Special Publication **184**.
- McLAREN S., SANDIFORD M. & HAND M. 1999. High radiogenic heat-producing granites and metamorphism—an example from the Mount Isa Inlier, Australia. *Geology* **27**, 679–682.
- MARK G. 2001. Nd isotope and petrogenetic constraints for the origin of the Mount Angelay Igneous Complex: implications for granitoid formation in the Cloncurry district, Australia. *Precambrian Research* **105**, 17–35.
- NORMAN M. D., PEARSON N. J., SHARMA A. & GRIFFIN W. L. 1996. Quantitative analysis of trace elements in geological materials by laser ablation ICPMS: instrumental operating conditions and calibration values of NIST glasses. *Geostandards Newsletter* **20**, 247–261.
- NOWELL G. M., KEMPTON P. D., NOBLE S. R., FITTON J. G., SAUNDERS A. D., MAHONEY J. J. & TAYLOR R. N. 1998. High precision Hf isotope measurements of MORB and OIB by thermal ionisation mass spectrometry: insights into the depleted mantle. *Chemical Geology* **149**, 211–233.
- O'DEA M. G., LISTER G. S., MACCREADY T., BETTS P. G., OLIVER N. H. S., POUND K. S., HUANG W. & VALENTA R. K. 1997. Geodynamic evolution of the Proterozoic Mount Isa terrain. In: BURG J.-P. & FORD M. eds. *Orogeny Through Time*, pp. 99–122. Geological Society of London Special Publication **121**.
- O'REILLY S. Y., GRIFFIN W. L. & BELOUSOVA E. A. 2004. TerraneChronTM: delivering a competitive edge in exploration. *Extended Abstracts SEG 2004*, pp. 145–148. Centre for Global Metallogeny, University of Western Australia Publication **33**.
- PAGE R. W. 1988. Geochronology of early to middle Proterozoic fold belts in northern Australia: a review. *Precambrian Research* **40/41**, 1–19.
- PAGE R. W. 1993. Geochronological results from the Eastern Fold Belt, Mount Isa Inlier. *AGSO Research Newsletter* **19**, 4–5.
- PAGE R. W., JACKSON M. J. & KRASSAY A. A. 2000. Constraining sequence stratigraphy in north Australian basins: SHRIMP U–Pb zircon geochronology between Mt Isa and McArthur River. *Australian Journal of Earth Sciences* **47**, 431–460.
- PAGE R. W. & SUN S.-S. 1998. Aspects of geochronology and crustal evolution in the Eastern Fold Belt, Mt Isa Inlier. *Australian Journal of Earth Sciences* **45**, 343–361.
- PAGE R. W. & SWEET I. P. 1998. Geochronology of basin phases in the western Mt Isa Inlier, and correlation with the McArthur Basin. *Australian Journal of Earth Sciences* **45**, 219–232.
- POLAT A., HOFMANN A. W., MÜNCKER C., REGELOUS M. & APPEL P. W. U. 2003. Contrasting geochemical patterns in the 3.7–3.8 Ga pillow basalt cores and rims, Isua greenstone belt, Southwest Greenland: implications for postmagmatic alteration processes. *Geochimica et Cosmochimica Acta* **67**, 441–457.
- POTMA W. A. & BETTS P. G. 2006. Extension-related structures in the Mitakoodi Culmination: implications for the nature and timing of extension and effect on later shortening in the eastern Mt Isa Inlier. *Australian Journal of Earth Sciences* **53**, 55–67.
- RYBURN R. J., WILSON I. H., GRIMES K. G. & HILL R. M. 1988. *Cloncurry, Queensland, 1:100 000 Geological Map Commentary*. Bureau of Mineral Resources, Canberra.
- SCHERER E., MUNKER C. & MEZGER K. 2001. Calibration of the lutetium–hafnium clock. *Science* **293**, 683–687.
- SCOTT D. L., RAWLINGS D. J., PAGE R. W., TARLOWSKI C. Z., IDNURM M., JACKSON M. J. & SOUTHGATE P. N. 2000. Basement framework and geodynamic evolution of the Palaeoproterozoic superbasins of north central Australia: an integrated review of geochemical, geochronological and geophysical data. *Australian Journal of Earth Sciences* **47**, 341–380.
- VERVOORT J. D. & BLICHERT-TOFT J. 1999. Evolution of the depleted mantle: Hf isotope evidence from juvenile rocks through time. *Geochimica et Cosmochimica Acta* **63**, 533–556.
- VERVOORT J. D., PATCHETT P. J., BLICHERT-TOFT J. & ALBARÈDE F. 1999. Relationship between Lu–Hf and Sm–Nd isotopic systems in the global sedimentary system. *Earth and Planetary Science Letters* **168**, 79–99.
- WALTERS S. G. 1998. Broken Hill-type deposits. *AGSO Journal of Australian Geology & Geophysics* **17**, 229–237.
- WILLIAMS P. J. 1998. An introduction to the metallogeny of the McArthur River–Mount Isa–Cloncurry minerals province. *Economic Geology* **93**, 1120–1131.
- WYBORN L. A. I. 1998. Younger *ca* 1500 Ma granites of the Williams and Naraku Batholiths, Cloncurry district, eastern Mt Isa Inlier: geochemistry, origin, metallogenic significance and exploration indicators. *Australian Journal of Earth Sciences* **45**, 397–411.

Appendix 1 Locations of sampling sites.

Sample	Site	Easting	Northing	Zone	Size fraction
P9686	1	461950	7576300	54	< 1 mm
P9687	1	495081	7610010	54	< 1 mm
P9687	2	494362	7612257	54	< 1 mm
P9687	3	493419	7614098	54	< 1 mm
P9688	1	483100	7658900	54	< 1 mm
P9689	1	500421	7658596	54	< 1 mm
P9689	2	494558	7662545	54	< 1 mm
P9690	1	488232	7684776	54	< 1 mm
P9690	2	488727	7684585	54	< 1 mm
P9690	3	491327	7679297	54	< 1 mm
P9691	1	478532	7697888	54	< 1 mm
P9692	1	471329	7716624	54	< 1 mm
P9693	1	419933	7757441	54	< 1 mm
P9693	2	429602	7755830	54	< 1 mm
P9694	1	415940	7788376	54	< 1 mm
P9694	2	413557	7776089	54	< 1 mm
P9694	3	424145	7774436	54	< 1 mm
P9695	1	422792	7815744	54	< 1 mm
P9695	2	422418	7812165	54	< 1 mm
P9695	3	421367	7808731	54	< 1 mm

SUPPLEMENTARY PAPER**Appendix 2** Zircons of the Eastern Succession of the Mt Isa Inlier.